Spring 2015

Biogeochemical Cycling in a Headwater Stream and Riparian Zone

A. Capri Gillam
Montana Tech of the University of Montana

Follow this and additional works at: http://digitalcommons.mtech.edu/grad_rsch

Part of the Biogeochemistry Commons, Geochemistry Commons, and the Hydrology Commons

BIOGEOCHEMICAL CYCLING IN A HEADWATER STREAM AND RIPARIAN ZONE

by

A. Capri Gillam

A thesis submitted in partial fulfillment of the

requirements for the degree of

Masters of Science in Geoscience:

Hydrogeology Option

Montana Tech

2015

Abstract

Several teams of researchers at multiple universities are currently measuring annual and seasonal fluxes of carbon dioxide and other greenhouses gases (nitrous oxide and methane) in riparian wetlands and upland forests in the Tenderfoot Creek Experimental Forest (TCEF), a subalpine watershed in the Little Belt Mountains, Montana. In the current thesis, the author characterized the geochemistry and stable carbon isotope composition of shallow groundwater, soil water, and stream water in upper Stringer Creek, near sites that are being investigated for gas chemistry and microbial studies. It was hypothesized that if methanogenesis were a dominant process in the riparian wetlands of upper Stringer Creek, then this should impart a characteristic signal in the measured stable isotopic composition of dissolved inorganic carbon in shallow groundwater.

For the most part, the major solute composition of shallow groundwater in upper Stringer Creek was similar to that of the stream. However, several wells completed in wetland soil had highly elevated concentrations of Fe^{2+} and Mn^{2+} which were absent in the well-oxygenated surface water. Use of sediment pore-water samplers (peepers) demonstrated a rapid increase in Fe^{2+} and Mn^{2+} with depth, most feasibly explained by microbial reduction of Fe- and Mn-oxide minerals. In general, the pH of shallow groundwater was lower than that of the stream. Since concentrations of CO_2 in the groundwater samples were consistently greater than atmospheric pCO_2, exchange of CO_2 gas across the stream/air interface occurred in one direction, from stream to air. Evasion of CO_2 partly explains the higher pH values in the stream. Microbial processes involving breakdown of organic carbon, including aerobic respiration, anaerobic respiration, and methanogenesis, explain the occurrence of excess CO_2 in the groundwater. In general, the isotopic composition of total dissolved inorganic carbon (DIC) decreased with increasing DIC concentration, consistent with aerobic and/or anaerobic respiration being the dominant metabolic process in shallow groundwater. However, a minority of wells contained high DIC concentrations that were anomalously heavy in $\delta^{13}C$, and these same wells had elevated concentrations of dissolved methane. It is concluded that the wells with isotopically-heavier DIC have likely been influenced by acetoclastic methanogenesis. Results from shallow groundwater wells and one of the peeper samplers suggest a possible link between methanogenesis and bacterial iron reduction.

Keywords: *carbon dioxide, carbon isotopes, groundwater chemistry, biogeochemical cycling, riparian zone, headwater stream, geoscience, subalpine forest, Tenderfoot Creek Experimental Forest*

Acknowledgements

First of all, I would very much like to thank my advisor, Dr. Chris Gammons, for sharing his knowledge and wisdom as well as helping guide me as a young professional. I would also like to thank Dr. Steve Parker and Dr. Glenn Shaw for their invaluable knowledge both academically and as members of my thesis committee.

I wish to extend my gratitude to Brian McGlynn from Duke University for introducing TCEF as a field site and for allowing us to sample his wells. I also thank Simon Poulson from the University of Reno for carbon isotope analyses, Heiko Langner (University of Montana) for help with ICP and IC analyses, and both Heidi Reed and Dustin Jensen (MT Tech students) for their assistance with field work.

Table of Contents

List of Tables

List of Figures

List of Reactions

Glossary of Terms

Term	Definition
DIC	Dissolved Inorganic Carbon
DOC	Dissolved Organic Carbon
Eh	Redox Potential
GW	Ground Water
FA	Filtered Acidified
FU	Filtered Unacidified
IC - Analysis	Ion Chromatography Analysis
ICP - AES	Inductively Coupled Plasma-Atomic Emission Spectroscopy
LDO	Luminescent Dissolved Oxygen
NSF	National Science Foundation
PQL	Practical Quantification Limit
RU	Raw-Unacidified
SC	Specific Conductivity (mV)
S.I.	Saturation Index
SW	Surface Water
SWL	Static Water Level
T1 – T7	Transects 1 through 7
T	Temperature (Celsius)
TCEF	Tenderfoot Creek Experimental Forest

1. Introduction

Researchers at Montana State University, Duke University, the University of Nebraska, the University of North Carolina, and North Carolina State University are currently investigating annual fluxes of carbon dioxide and other greenhouses gases (nitrous oxide, methane) into and out of different landscape types at the Tenderfoot Creek Experimental Forest (TCEF). This interdisciplinary effort, funded by the National Science Foundation (NSF), includes hydrologists, microbiologists, geochemists, and atmospheric chemists.

Montana Tech is teaming with the larger TCEF group to characterize the surface and groundwater chemistry including stable isotope compositions of shallow groundwater, soil water, and stream water near sites also being investigated for gas chemistry and microbiology.

The field site of most interest is the riparian zone of upper Stringer Creek, a second-order tributary near the headwaters of Tenderfoot Creek. Previous workers (B. McGlynn and others) have installed a network of gas, soil-water, and ground-water monitoring wells along transects across the creek, its fringing wetlands, and the surrounding upland forests.

1.1. Thesis Objective

The overall goal of the inter-university project at TCEF is to understand linkages between aqueous transport, soil moisture, and groundwater chemistry as they apply to microbial populations and processes that produce and consume greenhouse gases. As part of this larger ongoing project, the major objective of this thesis is to conduct a temporal survey of stream and groundwater geochemistry, including the stable isotopic composition of dissolved inorganic carbon, as a function of position within the Stringer Creek drainage. It is hypothesized that if methanogenesis is a dominant process in the riparian wetlands of upper Stringer Creek, then this should impart a characteristic signal in the measured stable isotopic composition of dissolved inorganic carbon in shallow groundwater.

1.2.   Description of the Field Area

Tenderfoot Creek Experimental Forest (TCEF) is located within the west-central part of the Little Belt Mountains, just west of Neihart, Montana in the Lewis and Clark National Forest. Established in 1961 by the US Department of Agriculture, TCEF was formally dedicated for watershed research and recently expanded to include aspects of ecosystem management (McCaughey 1996). The region is currently managed by the Rocky Mountain Station in Bozeman, Montana.

The greater Tenderfoot Creek watershed is subdivided into five local regions, which includes Stringer Creek watershed, the primary focus for soil and groundwater research. Stringer Creek drainage encompasses 554 ha, with elevation ranging from 1,990 to 2,429 meters. Stringer Creek feeds into Tenderfoot Creek, a tributary to the Smith River which is esteemed for its prized trout fishing, recreation, and contribution to the Missouri River. The field area is characteristic of Northern Rocky Mountain subalpine watersheds, hosting similar-age classes of lodge pole pine forests with mosaic patterns typical of fire-prone regions (McCaughey, 1996). Stringer Creek includes instrumentation of 84 groundwater wells along 7 transects progressing from the upstream wetland in the northeast to its drainage into Tenderfoot Creek in the southwest (Figure 1).
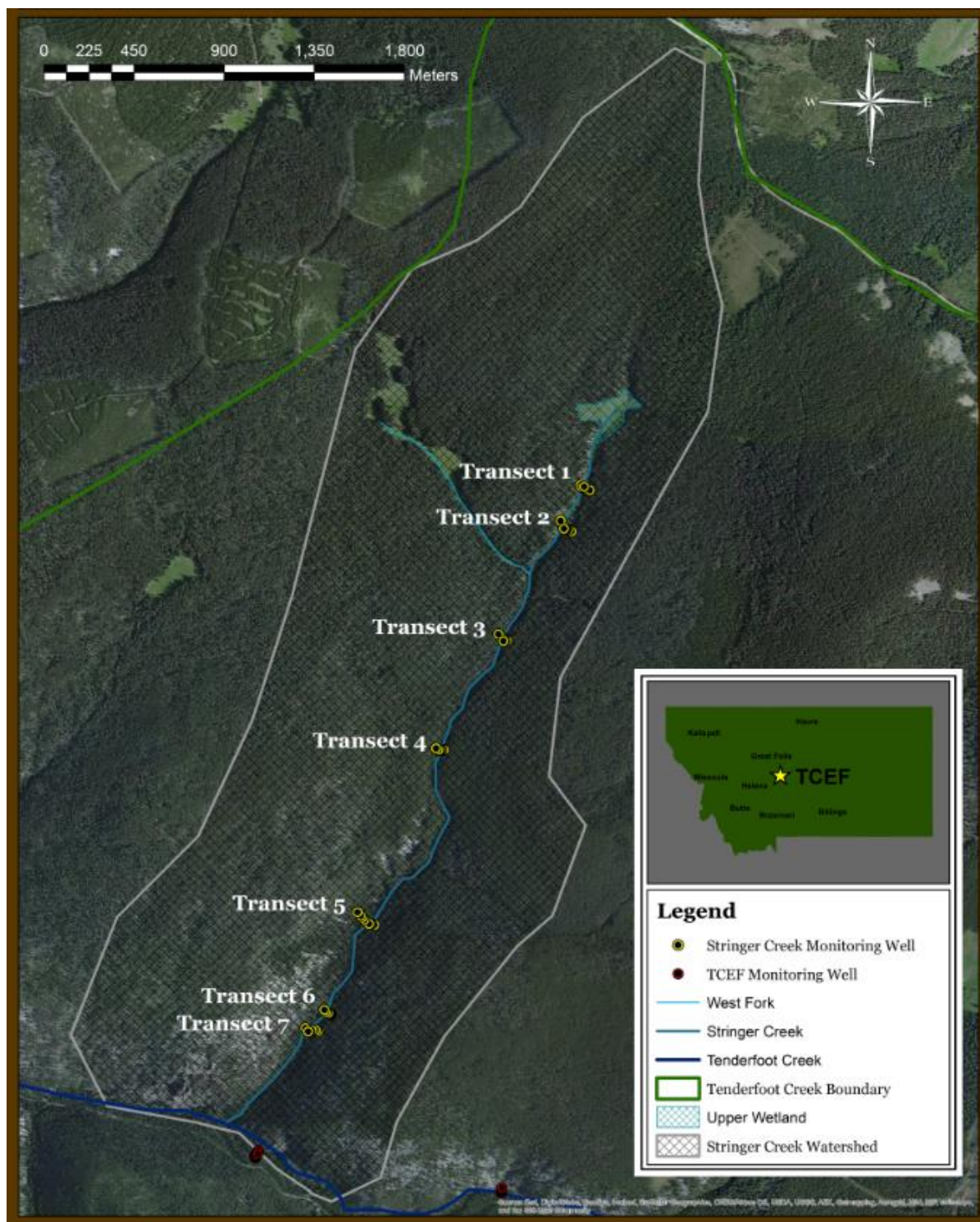
Figure 1: Location of monitoring well transects in Stringer Creek

1.3. Climate

Average annual precipitation for TCEF is 880 mm (34.6 in), and ranges with elevation

from 590 mm (23.2 in) to 1050 mm (41.2 in) (McCaughey, 1996). Peak precipitation occurs in

winter months (early November to late May), primarily as snow, and accounts for 70% of the

total annual precipitation. Annual runoff is estimated at 250 mm (9.8 in) per year, with much of

this occurring during snowmelt in late spring (late May to early June) when mountain soils are

typically saturated (McCaughey, 1996). Since summer thunderstorms are relatively rare,

overland flow and related soil erosion are typically associated with snowmelt.

Growing seasons are short at high elevations, and snow can occur at any month of the

year. TCEF has a mean annual temperature of 0°C, ranging from a daily average of -13°C in

January to 14°C in July (Farnes et al., 1995). Dry, south-facing slopes may experience soil

moisture stress, and killing frosts may additionally limit plant growth. Native plants experience

typical growing seasons of 30-75 days, depending on elevation, within TCEF (McCaughey,

1996).

1.4. Geology and Soils

Geological units within the TCEF region include Precambrian granitic gneiss, Cambrian

sedimentary rocks of the Flathead and Wolsey Formations, and Tertiary (Eocene) intrusions of

rhyodacite porphyry (Reynolds, 1995; Farnes et al., 1995, McCaughey, 1996). The distribution

of rock types is summarized in Figure 2 below (modified from Reynolds, 1995). Granitic gneiss

forms the basement rock of the Little Belt Mountains, and is the underlying foundation of lower

Stringer Creek. This crystalline rock offers limited pathways for groundwater flow through

fractures (Reynolds, 1995). The contact between Precambrian gneiss and Cambrian Flathead

Sandstone occurs between transects 4 and 5 in the Stringer Creek watershed, near a west flowing

drainage (Figure 1). The Flathead Sandstone is tightly cemented and has low permeability, with

the exception of weakly cemented laminae and fractures (Reynolds, 1995). The Flathead/ Wolsey boundary occurs in Upper Stringer Creek, upstream of transect 1. This is an area of perennial springs which increase in magnitude and number during snowmelt. Despite its low primary permeability, the Wolsey Shale has abundant secondary fractures which allows water to infiltrate in high-altitude areas of low relief, and from there, to move downslope along the Flathead/Wolsey contact, emerging as springs (Reynolds, 1995). Groundwater in contact with the Wolsey Fm. picks up bicarbonate alkalinity by dissolution of limestone concretions within the shale.

Soils in upper Stringer Creek are mainly derived from the Wolsey Shale, which weathers to form subdued slopes and clay-rich soil, and the Flathead Sandstone, which weathers to silica sand (Reynolds, 1995; Farnes et al., 1995). The Flathead Sandstone is locally rich in iron oxides which impart a pink, yellow, or reddish-brown color to the unit. Iron oxides also form from the weathering of mafic minerals (biotite and hornblende) within the upstream porphyritic rhyodacite and granitic gneiss along lower Stringer Creek (Reynolds, 1995; Farnes et al., 1995). Riparian soil is primarily clay with soil depths ranging from 1-2 m, while hill-slope soils contain more sands and silts ranging from 0.5 -1.0 m in depth (Jencso et al., 2009).
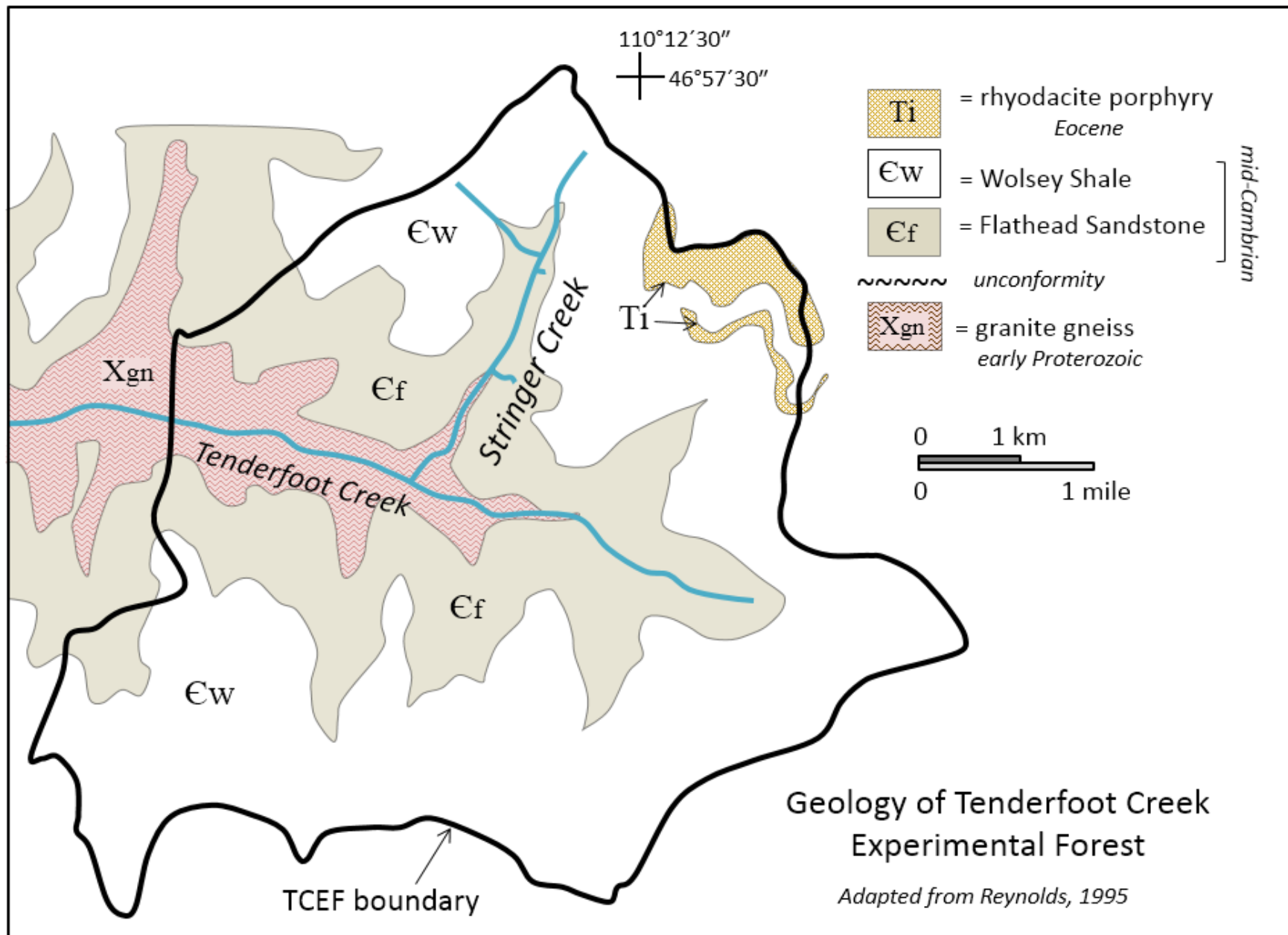
Figure 2: Geologic map of the Tenderfoot Creek field Area. Geology adapted from M. Reynolds (1995)

2. Methods

2.1. Field Methods

Seven sampling events were conducted in TCEF over a three year period from July 2012 to August 2014. Sampling visits in July of 2012 were conducted by C. Gammons and undergraduate student Heidi Reed, prior to the author taking on the project. Samples were collected during early-summer, mid-summer, and early fall seasons (Figure 3), and focused on seeps, streams, and shallow groundwater. Measurement sites were selected based on pre-existing groundwater instrumentation, as well as at sites specific to this study.

**Figure 3: Upper wetland of Stringer Creek in spring, summer and fall months
(June 2013, July 2013, and October 2013)**

Stringer Creek, which flows from the north to the south, includes well pairs along 7 transects. These established sites include groundwater wells on both the east (E) and west (W) sides. Wells were numbered sequentially with 1 being in closest proximity to the creek, while the highest number represented the furthest, most uphill site. At all transects, none of the wells with a number code greater than 4 ever contained enough water to collect a groundwater sample. Most groundwater samples were collected from within 0-30 m of the stream. Seeps and streams feeding into Stringer Creek were sampled based on seasonal flow. Table I summarizes the dates of field visits and types of data collected on each visit.

Table I: Dates of field visits and types of data collected

	2012		2013			2014	
	July 10-12	July 29-30	June 8-9	July 26-28	Oct. 5-6	July 27-28	Aug. 11
Groundwater samples	X	X	X	X	X	X	
Stream samples	X	X	X	X	X	X	
ICP-metals	X	X	X	X	X	X	
IC-anions				X		X	
DOC concentration					X	X	
Dissolved methane				X	X		
water isotopes	X		X				
DIC isotopes	X	X	X	X	X	X	
DOC isotopes						X	
Diel cycles in stream	X			X			
Peeper installed	X					X	
Peeper sampled		X					X
Transects Sampled	T1-T4	T5-T6	T1-T4	T1-T6	T1-T4	T1-T2	NA

2.1.1. Groundwater Well Sampling

Shallow wells from transects 1-6 were used to monitor groundwater and collect the samples listed in Table I. Wells consisted of 3.8 cm (1.5 in) inside-diameter PVC pipes with completion depths that varied from 1–1.5 m in the riparian zones and 0.5-1 m in the hillslopes (Pacific, 2009). Wells were first measured for static water level, then purged dry using a peristaltic pump and tubing. Initial parameters including temperature (T), specific conductivity (SC), pH, and luminescent dissolved oxygen (LDO) were recorded using a Hydrolab MS5, flow cell, and portable Surveyor (Figure 4). The Hydrolab was calibrated on the morning of each sampling day using standard pH and SC buffers and air-saturated water. All samples that needed to be filtered were transferred into a pre-rinsed 60-mL HDPE syringe to which a 0.2 μm PES syringe filter was attached. About 10-20 mL of water was passed through the filter and used to rinse the sample containers prior to filling.
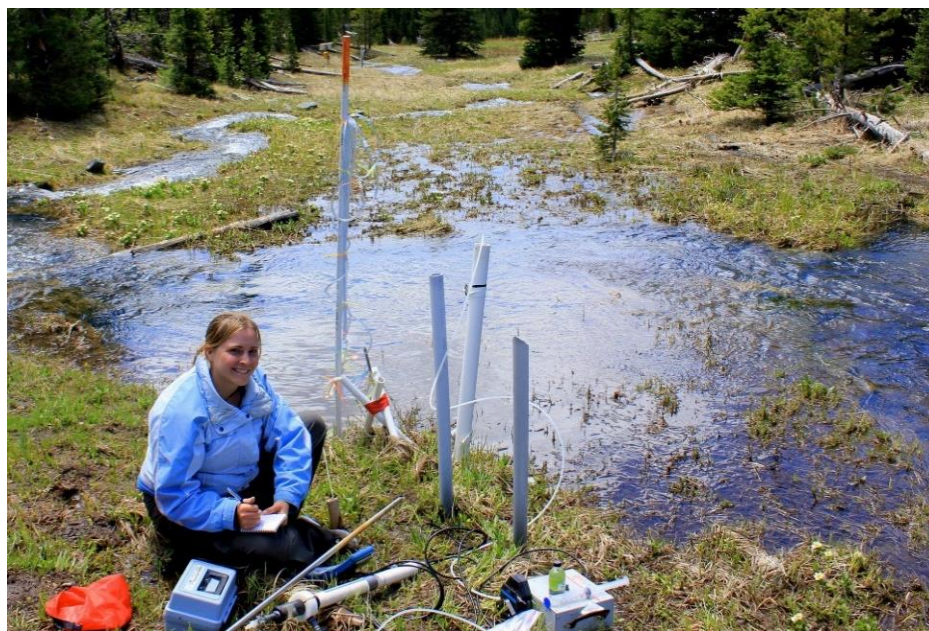
Figure 4: Groundwater well sampling June 2013

Most wells could not be continuously pumped, even with the peristaltic pump set at a low pumping rate (e.g., < 200 mL/minute) due to low productivity. During early visits, wells were re-measured regularly to help determine individual recovery times. After pumping dry, it took roughly 6 to 24 hours for the wells to recover, sometimes longer. The groundwater samples were often turbid (white, tan, or red-brown being the most common colors) and difficult to filter, so not all sample types could be collected during each visit, and occasionally less than ideal volumes of water were collected. For wells containing a high dissolved Fe content, the red color of the well water showed that the dissolved Fe in the well was oxidizing, and that the sample probably was not representative of the actual groundwater in the adjacent saturated wetland soils.

Beginning in 2013, an argon gas purge method was established to collect shallow groundwater samples. This involved measuring the static water level (SWL) and then pumping the well dry, taking a preliminary set of hydrolab readings during the process. 1 to 2 cubic feet of argon gas were then injected into the well, and the well was capped. Because argon is heavier than air, this created a buffer zone separating groundwater from oxygen in the atmosphere as the

well recovered. Later in the day, or more commonly the next day, the wells were revisited and pumped slowly to collect a second (final) set of hydrolab readings. The hydrolab was then disconnected and water samples were collected directly from the peristaltic pump outlet line.

Samples were collected in order of importance, with consideration to the difficulty of filtering and the volumes required. Filtered acidified (FA) samples were collected for ICP analysis (60 mL, 1% HNO_3) and filtered unacidified (FU) samples were collected for IC analysis (60 mL, unpreserved) and for water isotope analysis (10 mL glass bottle with conical lid). FA samples for ICP samples were acidified within 48 h to 1% v/v HNO_3 using trace metal grade purity HNO_3 acid. Samples for isotopic composition of dissolved inorganic carbon were collected in a 125 mL glass bottle (2012-2013 visits) or in a 40 mL glass bottle (2014 visits). At every well where DIC-isotope samples were collected, an alkalinity titration (100 mL) was performed in the field on a raw water sample. In addition to these procedures, some wells were sampled for DOC concentration and dissolved gas concentration. The latter samples were collected into 100 mL glass bottles with a rubber septum that had been pre-evacuated in the laboratory (see Smith et al., 2011 for more details). A small mass of mercuric-chloride was added to each gas bottle to minimize bacterial reactions after sampling. To fill the gas bottles, a needle connected to the peristaltic pump outlet line was inserted through the rubber septum. The gas bottle slowly filled with sample, leaving a small vapor bubble for later gas analysis. All samples were stored in a cooler containing ice prior to returning to the lab, at which time they were moved into a refrigerator.

2.1.2. Stream and Seep Sampling

Stringer Creek, along with miscellaneous seeps and tributary inflows, were sampled in a similar manner to the ground water wells along each transect. Field parameters were obtained using the Hydrolab, providing T, SC, pH, and LDO.   At most sites, a set of FA and FU samples

was collected, as well as samples for DIC and water isotope analysis. The methods outlined above were followed, except that it was not necessary to use the peristaltic pump and therefore water was sampled directly using a 60 mL plastic syringe.   Diel changes in field parameters (water temperature, pH, dissolved oxygen) in upper Stringer Creek were measured during July 2012 and July 2013 using a MS5 Hydrolab. Readings were collected every 0.5 h for 24 h. Data were later downloaded from the MS5 memory.

2.1.3. Peeper Sampling

Vertical gradients in pore-water chemistry in the top 0.5m of saturated soil were determined by deploying sediment pore-water samplers, also known as "peepers". The peepers used in this study were purchased from Rickly Hydrological, and are modifications of the original design proposed by Hesslein (1976). The peeper is a rectangular, acrylic sampler with 28 rows of horizontal sample compartments spaced 1 cm apart (Figure 5). A semi-permeable sheet of nylon (5 micron pore size) is used to separate the sample cells, which are pre-filled with de-oxygenated distilled water, from the outer acrylic shell, which is screwed tightly into the back of the peeper. The peeper is installed vertically into the saturated soil so that all sample chambers are wet. Over a period of 2-3 weeks, solutes in the sediment pore-water diffuse across the nylon membrane until the chemistry of the water in the sample chambers is the same as the chemistry of the pore water.   The peeper is then withdrawn from the soil, wrapped in a ziplock bag with a continuous flow of Ar or N_2 gas (to prevent oxidation from air), and sampled as quickly as possible following the procedures outlined below.

Figure 5: Peeper following collection period & sample suite

The first peeper was installed in July 2012 into a muddy "hole" in the dense wetland vegetation on the west side of Stringer Creek near Transect 2. Although no marker was present, this site could have been where a soil core sample had been previously extracted. Realizing that this may not be a good site to collect representative pore-water samples, the peeper was deployed as a test of how the method works. In July 2014, two more peeper samplers were installed into the wetland on the west side of Stringer Creek near transects 1 and 2.   This time care was taken to ensure that the peepers were driven into undisturbed soil.

Following a two week equilibration period, peepers were carefully removed and immediately wrapped in cellophane or a makeshift Ar/N$_2$ glovebag (essentially a large ziplock bag) to minimize gas loss and oxidation during sample collection. Each sampling event was guided using a peeper sampling plan (e.g. Figure 6). First, two microelectrodes (manufactured from Microelectrodes Inc.) were inserted directly through the nylon membrane into the sample cells to collect pH and Eh measurements. Each cell (either 5 mL or 10 mL volume) was used for a different purpose.   Sample types included: FA for ICP analysis; FU for anions or alkalinity; raw samples for phosphate, dissolved sulfide, or ammonium analysis. In each case, the mass of sample collected from the peeper was determined by weighing the bottles before and after sampling. Bottles for FA samples were pre-filled with 20 mL of de-I water + 0.3 mL of HNO$_3$.

Bottles for FU samples and ammonium or sulfide analysis were pre-filled with 20 mL of de-I water. Reagents for colorimetric analysis of ammonium and sulfide were added immediately after collection of the respective peeper samples to prevent oxidation. Samples for phosphate analysis were transferred directly into pre-weighed "Test-n-Tube" bottles provided by HACH Company, and reagents were added immediately after sampling.

ORDER	1	2	3	4	5	6	7	8
Cell	pH/ORP	ICP metals	SRP	H2S	NH4-N	As-speciation	alkalinity	IC-anions
1			A		B			
2								
3				A			B	
4								
5			A					B
6								
7				A	B			
8								
9			A				B	
10								
11				A				B
12								
13			A		B			
14								
15				A			B	
16								
17			A					B
18								
19				A	B			
20								
21			A				B	
22								
23				A				B
24								
25			A		B			
26								
27				A			B	
28								

(Left cell layout: 1a | 1b, 2 | 2, 3a | 3b, 4 | 4, 5a | 5b, 6 | 6, 7a | 7b, 8 | 8, 9a | 9b, 10 | 10, 11a | 11b, 12 | 12, 13a | 13b, 14 | 14, 15a | 15b, 16 | 16, 17a | 17b, 18 | 18, 19a | 19b, 20 | 20, 21a | 21b, 22 | 22, 23a | 23b, 24 | 24, 25a | 25b, 26 | 26, 27a | 27b, 28 | 28)

Figure 6: Example spreadsheet of peeper sampling parameters

2.2. Analytical Methods

A summary of analytical methods used in this thesis is given in Table II. Further details are outlined below.

Table II: Analytical methods, instruments and laboratories

Measurement	Instrument	Laboratory	Method	PQL[a]
pH	Microelectrode	Field	N/A	N/A
Sulfide	HACH 2010 Spectrophotometer	MT Tech	HACH 8131	0.01 mg/L as S
Phosphate	HACH 2600 Spectrophotometer	MT Tech	HACH 8048	0.01 mg/L as P
Ammonia	HACH 2010 Spectrophotometer	MT Tech	HACH 8038	0.02 mg/L as N
Alkalinity	Digital Titrator	Field	Potentiometric titration	N/A
Dissolved Organic C	Total C Analyzer	MBMG	Combustion	0.5 mg/L
Dissolved Organic C	Picarro C-isotope analyzer	MBMG	N/A	0.1 mg/L
Major and Trace Elements	ICP-AES	U-Montana	EPA 200.7	See Appendix B
Anions	IC	MT Tech or U-Montana	EPA Method 100.0	See Appendix C
Water Isotopes	IRMS	University of Nevada-Reno	N/A	N/A
Water Isotopes	Picarro Water Isotope Analyzer	MBMG	N/A	N/A
Dissolved Methane	Aurora-C & Picarro G-2131-I C-Stable Isotope Analyzer	MT Tech	N/A	N/A
δ13C-DIC	IRMS	University of Nevada-Reno	N/A	N/A
δ13C-DIC	Picarro C-Isotope Analyzer	MBMG	N/A	N/A
δ13C-DOC	Picarro C-Isotope Analyzer	MBMG	N/A	N/A

[a]PQL is the practical quantification limit for the instrumental method; N/A = not applicable.

2.2.1. Alkalinity

Alkalinity titrations were performed in the field using raw groundwater samples measured with a 100.0 mL graduated cylinder and transferred to a 250 mL Erlenmeyer flask where they were titrated to a pH 4.5 endpoint. While stirred continuously using a portable magnetic stirrer (or by hand when the stirrer malfunctioned), a HACH digital titrator with a 1.6 or 0.16 N sulfuric acid cartridge was used to adjust the pH of the water sample. The pH endpoint was determined using a bromcresol green-methyl red pH-indicator packet. Precision using this method was estimated at 2%, based on replicate titrations.

2.2.2. Ammonia

Filtered and refrigerated samples were analyzed for total dissolved ammonia (NH_4^+ + NH_3) within 24 hours of collection using a HACH portable spectrophotometer. The Nessler Method (HACH method 8038) was used, which is accurate for a range of 0.02 to 2.50 mg/L NH_3 as N. Waste from this procedure contains mercury and was therefore treated as hazardous waste. The colorimeter was zeroed with a solution of deionized water to which the HACH reagents were added. Calibration was checked during each analytical session by running at least one standard solution containing 0.1 to 1.0 mg/L NH_3 as N.

2.2.3. Phosphate

Filtered and refrigerated samples were analyzed for soluble reactive phosphate (PO_4^{3-}) within 24 hours of collection using a HACH portable spectrophotometer. The PhosVer 3 method (HACH Method 8048) was used with Test-n-Tube vials. This method is accurate for concentrations of phosphate in the range of 0.01 to 1.6 mg/L PO_4^{3-} as PO_4^{3-}. The instrument was calibrated during each session using at least one freshly prepared PO_4^{3-} standard.

2.2.4. Dissolved Methane

CH$_4$ concentrations in water samples were measured with an Aurora carbon analyzer (1030W) in conjunction with a Picarro G-2131-i C-stable isotope analyzer (cavity ring-down spectroscopy; CRDS). Reference solutions for calibration were generated by bubbling CH$_4$ through water in a closed vial to produce a saturated solution. The CH$_4$ concentration of this solution can be calculated based on the known solubility of CH$_4$ (Wiesenburg and Guinasso Jr., 1979). Several dilutions of the saturated solution were used to verify the accuracy of the concentration reported in the instrument data file. The estimated error based on duplicate determinations was less than 5 %.

2.2.5. ICP-metals

FA samples for quantification of major and trace elements were analyzed via Inductively Coupled Plasma-Atomic Emission Spectroscopy (ICP-AES) at the Biogeochemistry Laboratory at the University of Montana. EPA method 200.7 was used, which includes a lab blank, a lab duplicate, a lab spike, and a continuing calibration standard every 10 samples.

2.2.6. Anions/ Ion Chromatography (IC Analysis)

Select samples from July 2013 and July 2014 were analyzed for a suite of anions by ion chromatography (IC) at either the University of Montana Environmental Biogeochemistry Laboratory or Montana Tech at the MBMG laboratory. Shipped samples were transported in a cooler with ice packs, and the samples were analyzed within two weeks of collection. No preservative was added to the bottles. Filtered unacidified samples were collected for major anions analysis by Ion Chromatography (Dionex IC, EPA method 300.0) at Montana Tech. Anions analyzed were fluoride, sulfate, nitrite, nitrate, chloride, bromide, and phosphate.

2.2.7. Stable isotopes of DIC and DOC

All samples collected in 2012 and 2013 were processed for analysis of δ^{13}C-DIC following a modification of the method of Harris et al. (1997). Several mL of concentrated SrCl$_2$-NH$_4$OH solution were added to each DIC sample, which induced precipitation of DIC as SrCO$_3$. After several days, the solution was filtered and the SrCO$_3$ precipitate rinsed several times with deionized water. The filtered solid was then dried in an oven at 60°C overnight, transferred to a small glass vial, and sent to Dr. Simon Poulson at the University of Nevada, Reno for isotopic analysis. For some samples with low DIC concentration (e.g., < 30 mg/L), the mass of SrCO$_3$ recovered via this process was too small for an isotopic analysis. At Reno, the δ^{13}C of the SrCO$_3$ was measured by Dr. Poulson using a Eurovector elemental analyzer interfaced to a Micromass Isoprime stable isotope ratio mass spectrometer.

Samples collected in 2014, including a set of peeper samples from transects 1 and 2, were analyzed by Dr. Steve Parker at Montana Tech for concentrations of dissolved inorganic carbon (DIC) and dissolved organic carbon (DOC), as well as δ^{13}C-DIC and δ^{13}C-DOC. A Picarro G2131-i CRDS carbon isotope analyzer with an Aurora 1030W TIC/TOC analyzer was used for aqueous samples. Concentration standards were analyzed alongside the samples (Li$_2$CO$_3$, Na$_2$CO$_3$ and NaHCO$_3$ for inorganic C; Sucrose and potassium hydrogen phthalate (KHP; KC$_8$H$_5$O$_4$) for organic C). Carbon isotopic analysis was calibrated using the standards USGS 40 (glutamic acid, δ^{13}C= -26.39), USGS 41 (enriched glutamic acid, δ^{13}C=+37.63), and CH-6 (sucrose, δ^{13}C=-10.449). Analyses usually consisted of a standard bracketing every 10 samples. All isotope values were corrected based on a linear relationship between the CRDS reported value and the standard. All isotope values in this thesis are reported in units of per mil (‰) in the usual delta (δ) notation versus VSMOW for oxygen and hydrogen, and VPDB for carbon.

2.2.8. Stable Isotopes of water

One set of samples from July 2012 were analyzed by Dr. Simon Poulson at the University of Nevada-Reno for $\delta^{18}O$ and δD of water using a Micromass Isoprime stable isotope ratio mass spectrometer (IRMS) interfaced to either a Micromass MultiPrep device or a Eurovector elemental analyzer. Samples for $\delta^{18}O$-H_2O and δD-H_2O were analyzed after Epstein and Mayeda (1953) and Morrison et al. (2001), and have estimated precision of ±0.1‰ and ±1‰, respectively.

A second set of analyses (samples collected in 2013) was performed at Montana Tech used a Picarro L1102-i CRDS water isotope analyzer for $\delta^{18}O$-H_2O and δD-H_2O. Isotopic analysis for water at Montana Tech was calibrated using isotopic standards USGS 47 ($\delta^{18}O$ = -19.8; δD = -150.2), USGS 48 ($\delta^{18}O$ =-2.224; δD =-2.0) and VSMOW ($\delta^{18}O$ = 0.0; δD = 0.0). Analyses usually consisted of a standard bracketing every 10 samples. All isotope values were corrected based on a linear relationship between the CRDS reported value and the standard. The slopes for these calibrations were generally close to 1 (e.g., 0.98 to 1.01) with small offset correction.

2.3. Modeling and Data Interpretation

2.3.1. Visual MINTEQ

The program Visual Minteq (v. 3.0b, Gustafsson, 2010) was used to speciate dissolved inorganic carbon for each water sample between carbonic acid (H_2CO_3), bicarbonate (HCO_3^-) and carbonate ion (CO_3^{2-}). To do this, the sample pH, temperature, and alkalinity were input, along with approximate values of Ca^{2+} to help with charge balance. Visual Minteq also calculated the partial pressure of CO_2 (g) for each sample. Visual Minteq was also used to compute mineral saturation indices for selected groundwater samples for which complete chemistry (field parameters, cations and anions) was available.

3. Results

3.1. Water chemistry

All of the shallow groundwaters and streams sampled in this study had a near-neutral or slightly acidic pH (Figure 7A), with generally low SC values (Figure 7B). The average pH of groundwater wells and springs were similar (6.2 ± 0.3, 6.5 ± 0.4), both being less than the average pH of the streams (6.9 ± 0.3). In terms of SC, the groundwater and springs differed somewhat. Groundwater typically had a higher SC than the springs (82.6 ± 46.0, 55.2 ± 22.4), while springs and streams (55.9 ± 17.0) were similar. Some groundwater samples had anomalously high SC values, > 100 μS/cm. These high-SC wells were typically located in the wetlands near T1, T2, or T6 (early spring).
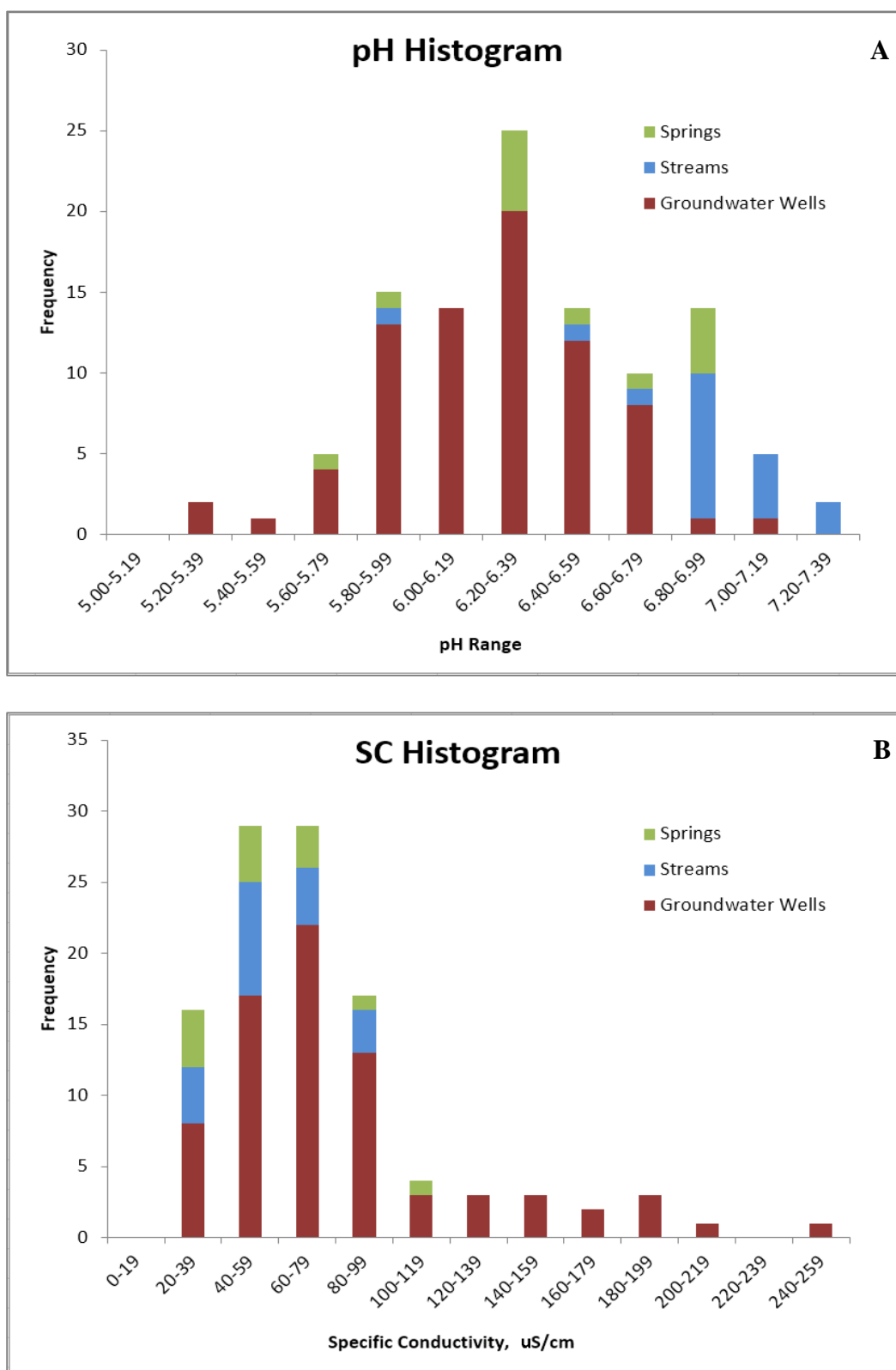
Figure 7: pH and SC histograms
(samples from 2012-2014)

Figure 8 summarizes the concentrations of major cations (Ca^{2+}, Mg^{2+}, Na^+, K^+, Fe^{2+}, Mn^{2+}) and anions (SO_4^{2-}, HCO_3^-) for samples collected in July 2012. Data from other seasons show very similar trends, but are omitted here for clarity. Overall, the data show similar chemical profiles between the groundwater wells and Stringer Creek (bold blue and red lines), with the exception of Fe^{2+} and Mn^{2+}. These solutes are absent from Stringer Creek, but show variable concentration in the groundwater, from below detection to > 100 µmol/L. In general, groundwater samples that had elevated Fe^{2+} concentrations were also enriched in Mn^{2+}.
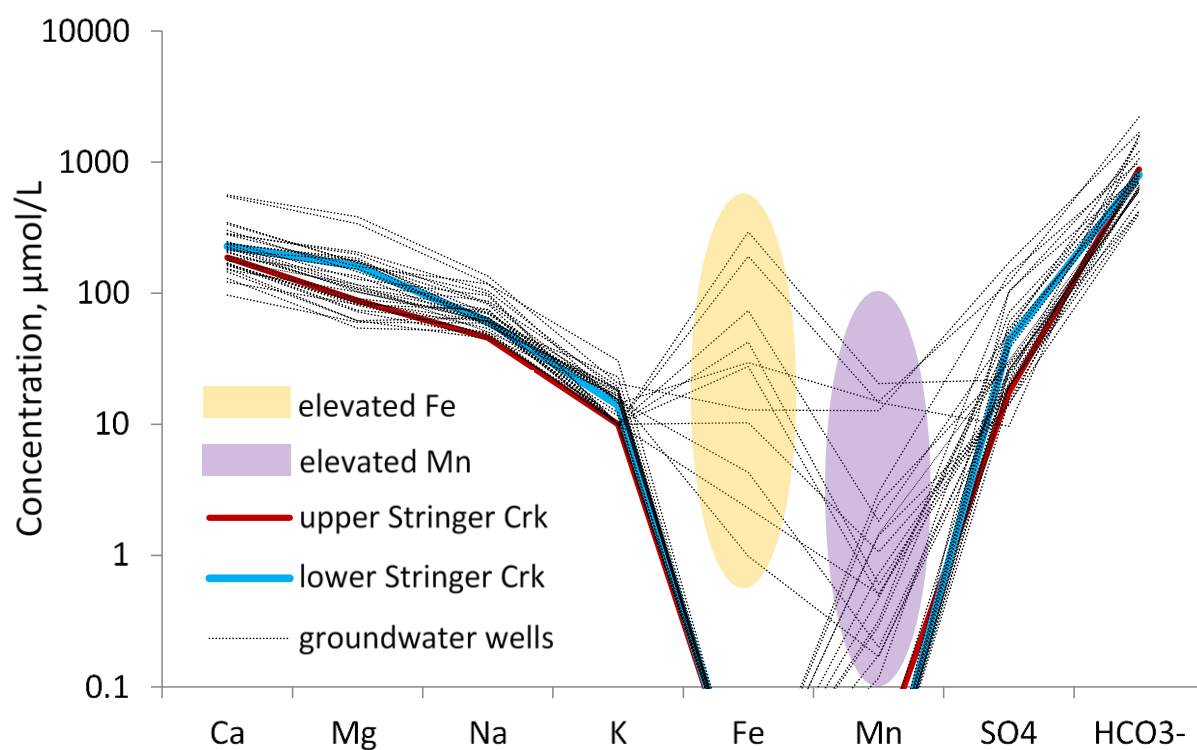
Figure 8: Comparison of major cations and anions in groundwater wells to upper and lower stringer creek. Areas of elevated Fe and Mn occur in wetland areas (2012 samples)

Figure 9 plots Eh vs. pH for all of the groundwater samples collected in this study for which ICP metals data were available. The diagrams were constructed using the program Stabcal (Huang, 2010) assuming total dissolved S, C, and Fe/Mn concentrations of 10 mg/L, 50 mg/L, and 1 mg/L, respectively. The shaded regions in Figure 9A show the stability fields of the solid phases ferrihydrite ($Fe(OH)_3$), siderite ($FeCO_3$), and pyrite (FeS_2). The shaded solids in 9B are rhodochrosite ($MnCO_3$) and the Mn-oxides. These fields will shrink or expand in size if the concentrations of dissolved S, C, Fe or Mn are changed from the values given above. Although each water sample has its own unique value of dissolved S, C, and metal concentrations, it is useful to look at all of the data simultaneously on a single diagram. Referring to Figure 9A, it appears that the Eh and pH of the groundwater is buffered near the dissolved $Fe^{2+}/Fe(OH)_3(s)$ boundary. In addition, some samples with higher pH are getting close to the stability field of siderite. In contrast, none of the samples had Eh values low enough to come close to the pyrite stability field. This agrees with the fact that none of the water samples had a noticeable smell of hydrogen sulfide, H_2S. Figure 9B indicates that all of the samples were in the field of dissolved Mn^{2+}, and were never close to saturation with any Mn-bearing solids.
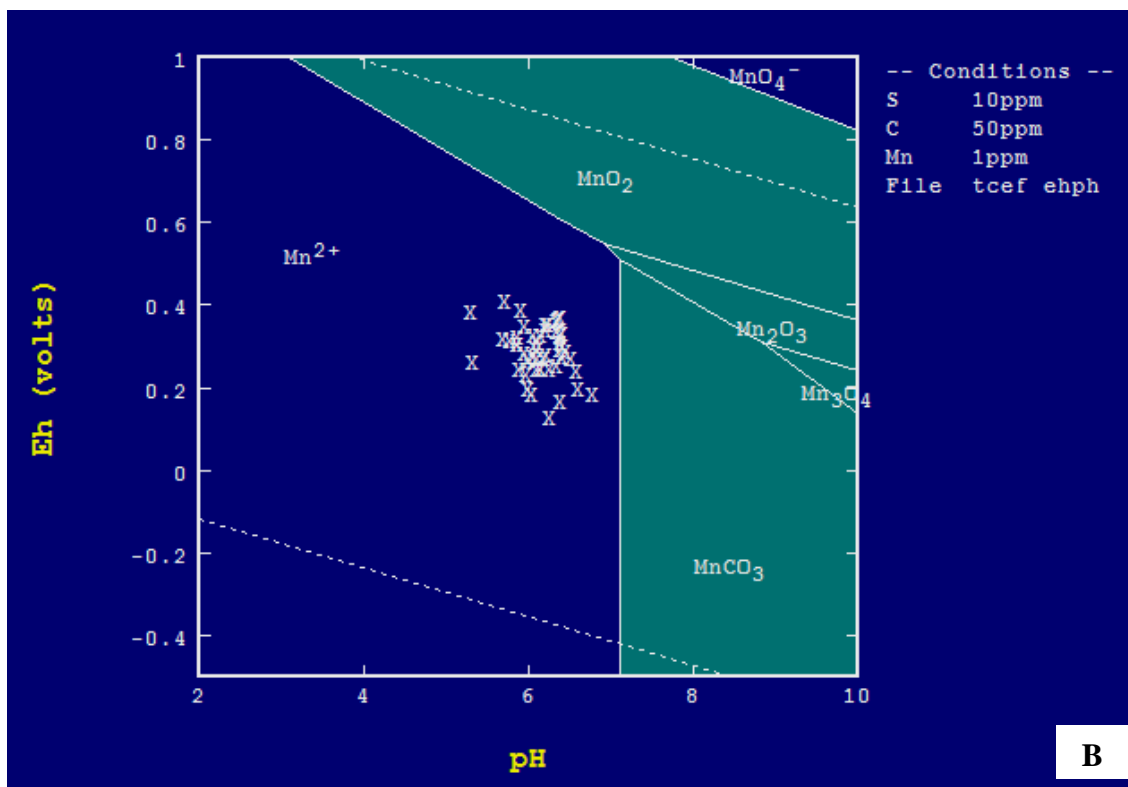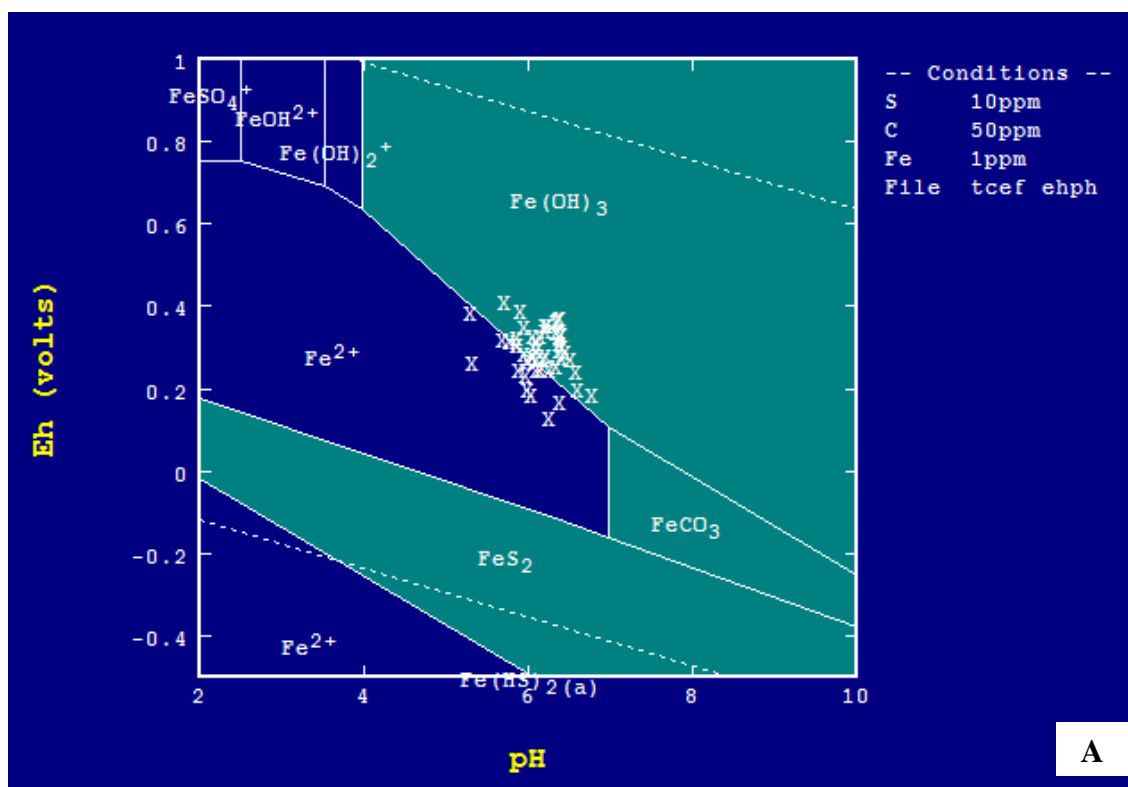
Figure 9: Eh-pH diagrams showing iron and manganese speciation in groundwater wells

3.1.1. Peeper Data

Changes in the concentrations of selected solutes with depth from the three peeper experiments are shown in Figure 10. In general, the first peeper (Peeper 0) showed very few trends in chemistry with depth. This is attributed to the fact that this peeper was installed into a "muddy hole" in the wetland vegetation, and consequently showed no gradients in pore-water chemistry. In contrast, Peepers 1 and 2, both of which were installed into firm, wetland soil, show distinct increases in the concentrations of dissolved Fe, Mn, Ca, and Mg with depth. Peeper 2 was deployed in an area of the T1 wetland that showed obvious Fe-oxide staining, and the sediment-pore water at this location contained over 100 mg/L Fe at a depth of 20 to 30 cm below surface (Figure 11A).   Some of the increase in solute concentration with depth in Peepers 2 and 3 could have been caused by loss of water to plant transpiration, a process that is known to influence the concentration of solutes in near-surface soil water (Drever, 1995). However, the magnitude of increase in Fe and Mn is too great in the case of Peepers 1 and 2 to be explained by this process, and must instead be the result of redox reactions occurring in the wetland soils.
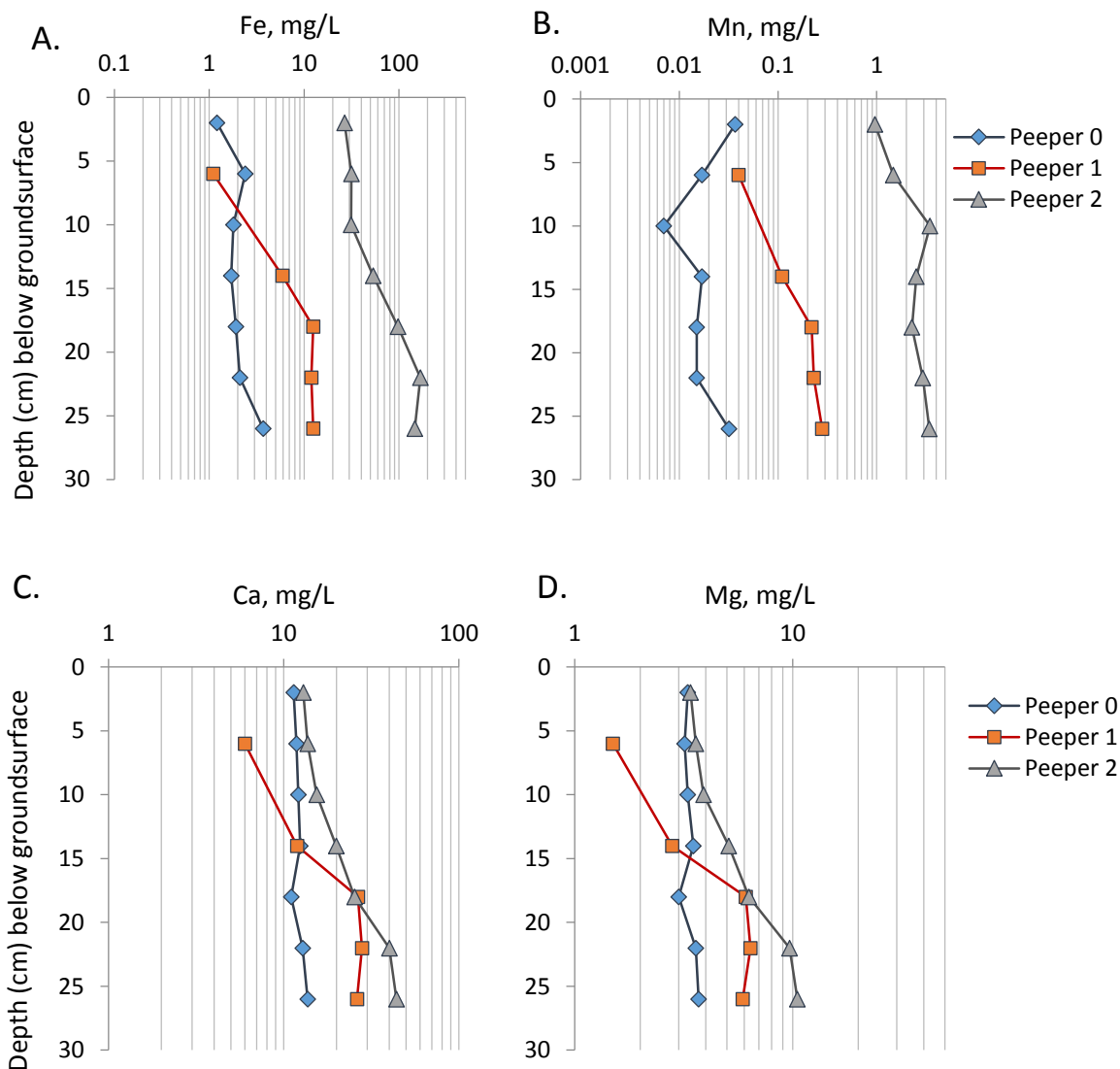
Figure 10: Changes in concentration of dissolved Fe, Mn, Ca, and Mg with depth in the peeper samples. See Appendix B for more information.

3.1.2. 24-Hour Hydrolab Data

Diel measurements of field parameters (water temperature, pH, SC, and dissolved oxygen) were

obtained over a 36-hour period in Stringer Creek near Transect 2 in July 2012 and again in July

2013 (Figure 11 below). Both July 2012 and 2013 data presented similar results where peak

temperature occurred around 16:00, nearing 11.5°C. The 24-h change in pH was 0.5 pH units on

July 11 and 0.3 units on July 12, with maximum values in early afternoon and minima at night.

Temperature followed similar trends as pH (Figure 11B). Dissolved oxygen varied in an inverse fashion to pH and temperature, with a maximum concentration in the morning and a minimum in the early evening. Referenced to atmospheric saturation, the DO values were at 100% to 110% of saturation over the entire monitoring period. The slight decreases in DO concentrations during the day were most likely caused by an increase in stream-water temperature, keeping in mind the retrograde solubility of O_2 in water. The relatively small magnitude in diel ranges for pH and DO are consistent with upper Stringer Creek being a clear, swift-moving headwater stream with low nutrient loads. The small diel cycles also mean that samples collected from the creek for DIC concentration and isotopic composition should give similar results irrespective of the time of day. This is not the case for streams that have high biological productivity, as has been shown in preceding research (Parker et al., 2005, 2010).
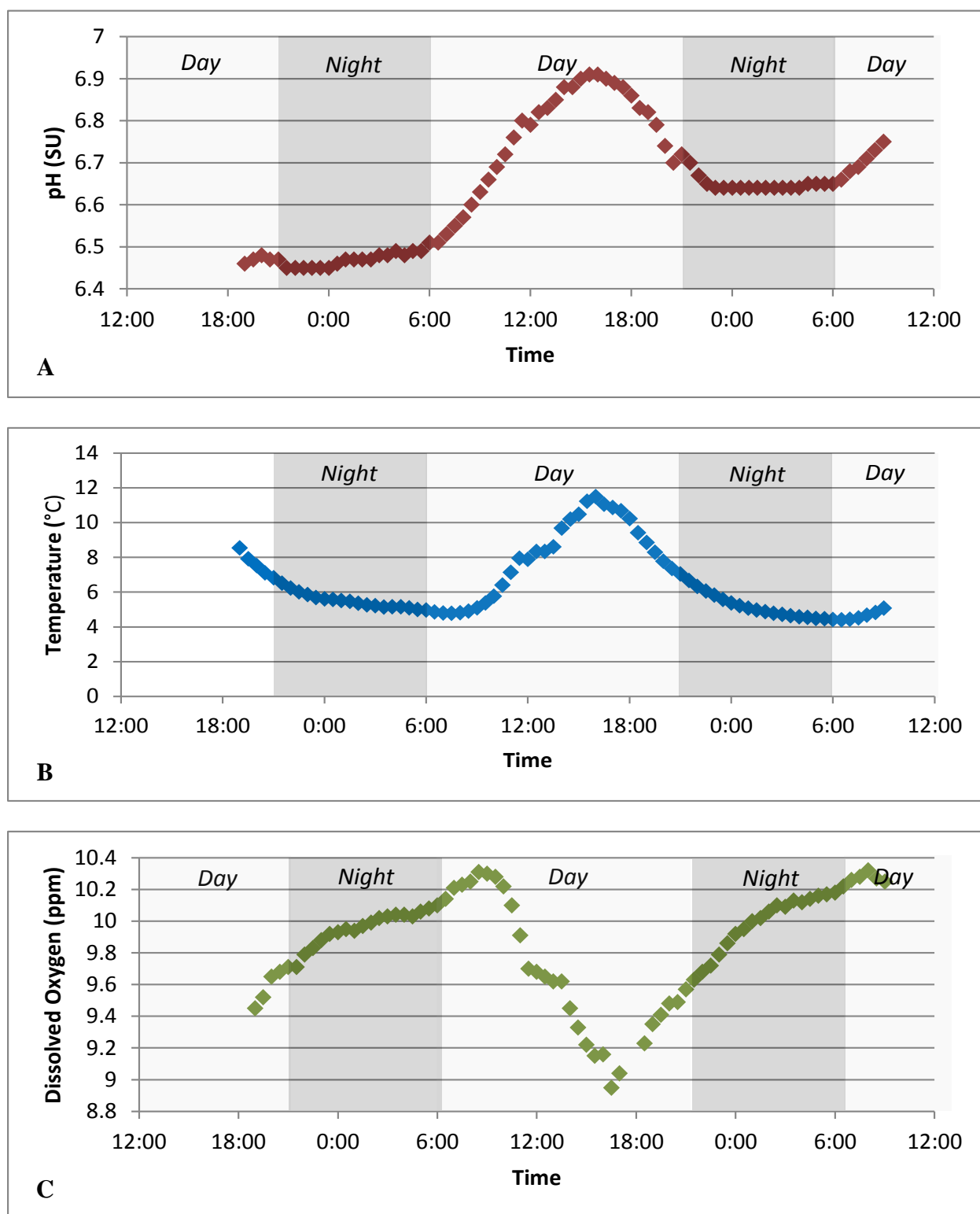
Figure 11: 24-Hour Hydrolab Data (Collected July 2012)

3.1.3. Dissolved Methane Analyses

A subset of groundwater samples collected from transects T1 to T6 was analyzed for dissolved methane at Montana Tech in July and October of 2013. Because of the difficulty in collecting representative samples of groundwater from many of the wells, most of which could not be pumped continuously during sampling, these data should be interpreted with caution. Nonetheless, the results show elevated methane in most of the groundwater samples collected, with the highest values in the wetland piezometers of Transects 1 and 2.

Table III: Dissolved methane results

Date	Location	Dissolved CH$_4$, µM	Date	Location	Dissolved CH$_4$, µM
7/27/2013	T1E1	39.6	10/5/2013	Bedrock	BD
7/27/2013	T1W1	39.4	10/6/2013	T1W1	53.8
7/27/2013	T2E1	23.6	10/6/2013	T1W2	BD
7/27/2013	T2W1	32.3	10/6/2013	T2E1	7.5
7/27/2013	T2W3	21.6	10/6/2013	T2W1	BD
7/27/2013	T3E2	32.8	10/6/2013	T3E2	BD
7/27/2013	T4E2	4.6	10/6/2013	T3E2 dup	BD
7/27/2013	T6E1	7.6	10/6/2013	T4E2	8.6
7/27/2013	T6W1	BD	10/6/2013	T4W1	7.3

3.1.4. Dissolved Organic Carbon Analyses

Dissolved organic carbon (DOC) was measured in a subset of samples on two occasions, the first being in October 2013, and the second in July 2014. The first set of samples (measured by the Montana Bureau of Mines and Geology laboratory) showed a range of 0.2 to 6.9 mg/L DOC (see data in Appendix F), with the lowest value coming from the "Bedrock Well", and the highest from T2W1. The second set of samples (measured at Montana Tech using the Picarro C-isotope analyzer) gave a more narrow range of 0.7 to 2.0 mg/L DOC, with the highest value coming from T1E1.

3.2. Stable Isotopes

3.2.1 Water isotopes

Data on the stable O- and H-isotope composition of water are tabulated in Appendix D, and summarized in Figure 12. All samples of shallow groundwater and stream water plot near the global meteoric water line of Craig (1961) and the meteoric water line for Butte, Montana (Gammons et al., 2005).   None of the samples show evidence of evaporation. In general, 2013 experienced a colder spring with higher snow cover compared to 2012. The colder and wetter spring could explain the observation that most of the 2013 samples were isotopically lighter than most of the 2012 samples. The fact that the July 2012 and June 2013 samples are displaced suggests that the mean residence time of groundwater in the watershed is short (< 1 year). However, the two sets of data were collected by different laboratories using different methods, so it is possible that the apparent offset between 2012 and 2013 data is an artifact of analytical error.
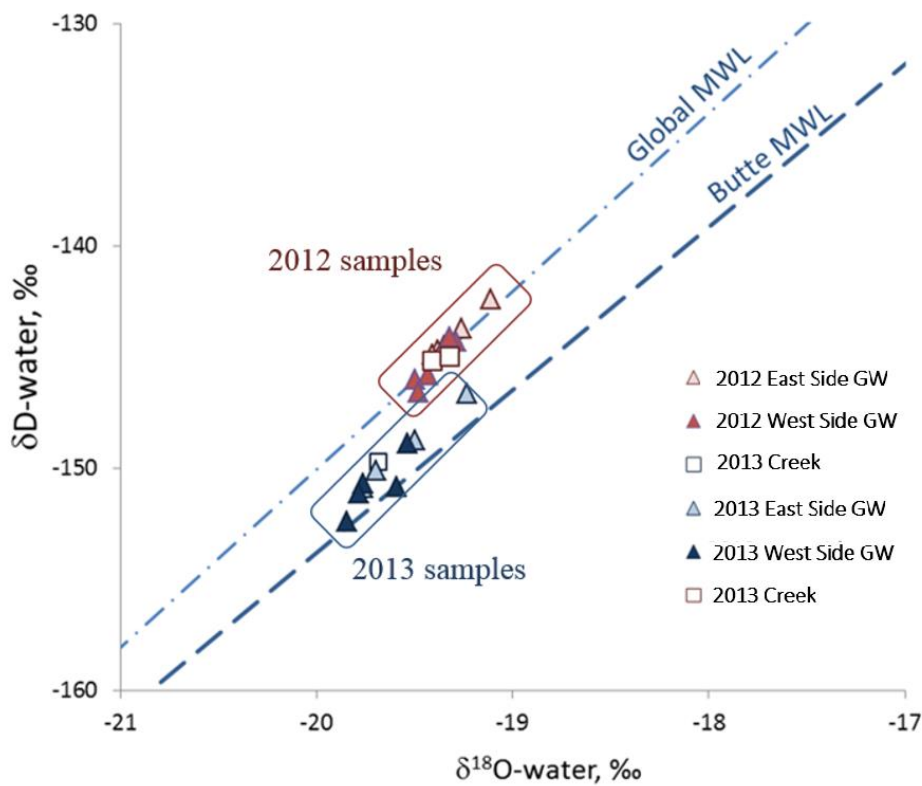
Figure 12: 2012-2013 Water Isotope Data

3.2.2. DIC isotopes

Data on the concentrations and isotopic compositions of dissolved inorganic carbon (DIC) for 66 samples of stream water, shallow groundwater, and spring water are tabulated in Appendix E. Additional data on dissolved carbon concentrations and isotopic compositions are given for the two peepers deployed in July of 2014 (see Appendix F). An interpretation of these data is given in the discussion section of this thesis.

3.2.3. DOC isotopes

Seven samples of stream and shallow groundwater collected in July of 2014 were analyzed for δ^{13}C-DOC using the Picarro C-isotope analyzer at Montana Tech. The results (Appendix F) show a narrow range in δ^{13}C from -28.1 to -32.7 ‰ (average = -31.1±1.4, one standard deviation). These results show that the DOC in the Stringer Creek area is isotopically light, with a range in values that is typical of DOC in terrestrial waters that are dominated by C_3 plants (Clark and Fritz, 1997).

4. Discussion

4.1. General Trends in Water Chemistry

As shown in Figure 13 below, concentrations of CO_2 in the groundwater samples were always much greater than atmospheric pCO_2 concentrations (roughly 0.0003 atm at the elevation of upper Stringer Creek), approaching 0.1 atm in the well samples with lowest pH. Figure 13 also shows a near-linear, inverse relationship between pCO_2 and pH. This relationship stems from the influence that CO_2 has on pH, through the first dissociation constant of carbonic acid, $H_2CO_3(aq)$:

$$CO_2(g) + H_2O(l) \leftrightarrow H_2CO_3(aq) \leftrightarrow H^+ + HCO_3^- \qquad (I)$$
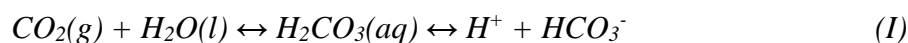
Most of the CO_2 in the groundwater well samples is probably coming from reactions involving the microbial breakdown of organic carbon, including aerobic respiration, anaerobic respiration, and methanogenesis. Example reactions are given here:

$$CH_2O(s) + O_2 \rightarrow CO_2 + H_2O \qquad (II)$$

$$CH_2O(s) + 4Fe(OH)_3(s) + 8H^+ \rightarrow 4Fe^{2+} + CO_2 + 11H_2O \qquad (III)$$

$$CH_3COOH(aq) \rightarrow CH_4 + CO_2 \qquad (IV)$$
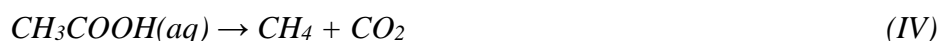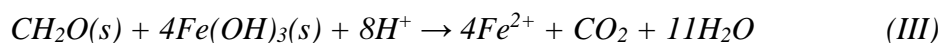
Reaction II summarizes aerobic respiration of organic carbon (CH_2O), and is essentially the reverse of photosynthesis. Reaction III is one of several possible anaerobic respiration reactions, in this case involving reduction of ferric iron (Fe-hydroxide) to soluble Fe^{2+}. Similar reactions could be written for reduction of nitrate and nitrite to $N_2(g)$, Mn-oxides to Mn^{2+}, and sulfate to hydrogen sulfide (H_2S). Reaction IV is the acetoclastic methanogenesis reaction, wherein acetic acid (CH_4COOH) is converted to a 1:1 mixture of CH_4 and CO_2.
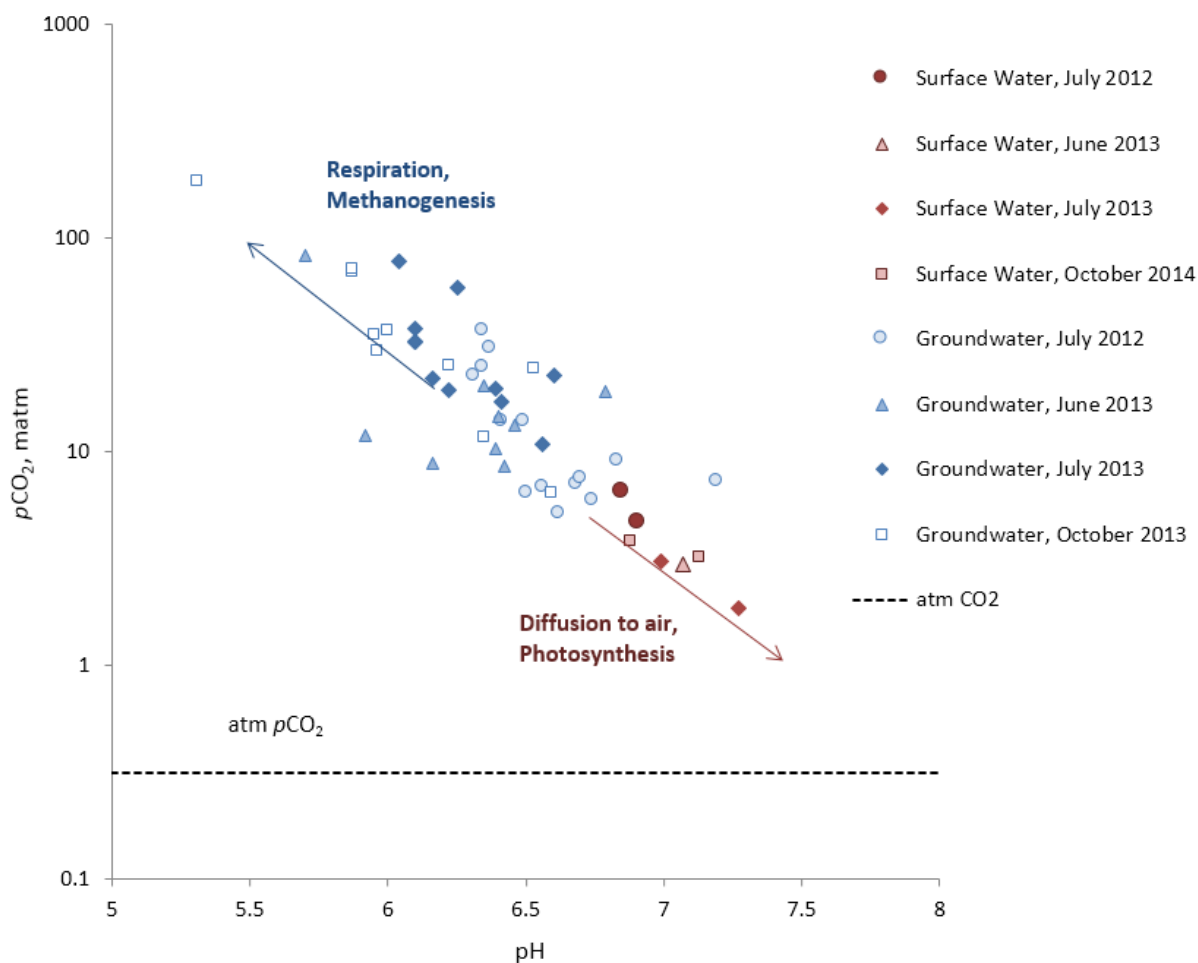
Figure 13: pH vs pCO₂ Diagram

After emerging at the surface as a spring or stream, dissolved CO_2 begins to evade to the atmosphere, causing an increase in pH. During the day, photosynthetic consumption of dissolved CO_2 by aquatic plants also causes an increase in pH in the stream, especially in mid-summer when plant and algal growth is high. This is reflected in the higher pH values of upper Stringer Creek recorded during the afternoon hours (see Figure 11 above). Despite the effects of diffusion and photosynthesis, the data in Figure 13 show that Stringer Creek and its tributaries always had pCO₂ values greater than atmospheric values. For this reason, any exchange of CO_2 across the stream/air interface would have always occurred in one direction, that is, from stream to air.

Figure 14 below takes a closer look at the relationship between SC and pH. As shown in the lower scatter plot, all groundwater samples with SC > 100 μS/cm also contained measureable concentrations of dissolved Fe^{2+}. At the pH values of the water samples, concentrations of Fe^{2+} greater than 0.1 mg/L can only be achieved if the water is anoxic. If present, dissolved O_2 would rapidly oxidize Fe^{2+} to Fe^{3+}, which, at pH > 4, would precipitate out as some form of insoluble oxy-hydroxide solid, such as amorphous $Fe(OH)_3$, ferrihydrite, or goethite (FeOOH). An area roughly 10 m x 5 m in size of visible iron-oxide staining exists upstream of Transect 1, and smaller Fe-rich seeps and springs can be seen at certain times of the year further downstream. It is possible that the Fe-rich groundwater obtained its distinct chemistry in situ, that is, within the shallow wetland soils bordering the creek. If so, reactions II and III probably would have played a major role in buffering the groundwater chemistry. It is also possible that some of the high-Fe and high-SC water represents groundwater that is discharging along a deeper flow path, perhaps through fractures in the Flathead Sandstone or overlying Wolsey Shale. Outcrops of Flathead Sandstone near TCEF vary in color from pale yellow to deep red-brown, indicating the presence of iron oxides. If conditions were anoxic, these iron minerals could be dissolved into groundwater as it makes its way through the fractured bedrock. However, evidence weighing against this idea is the fact that groundwater pumped from the "bedrock well" at Transect 1, which was completed several meters into the Flathead Sandstone, is not particularly high in SC (92 μS/cm), and contains no detectable Fe^{2+} (see data in Appendix A).
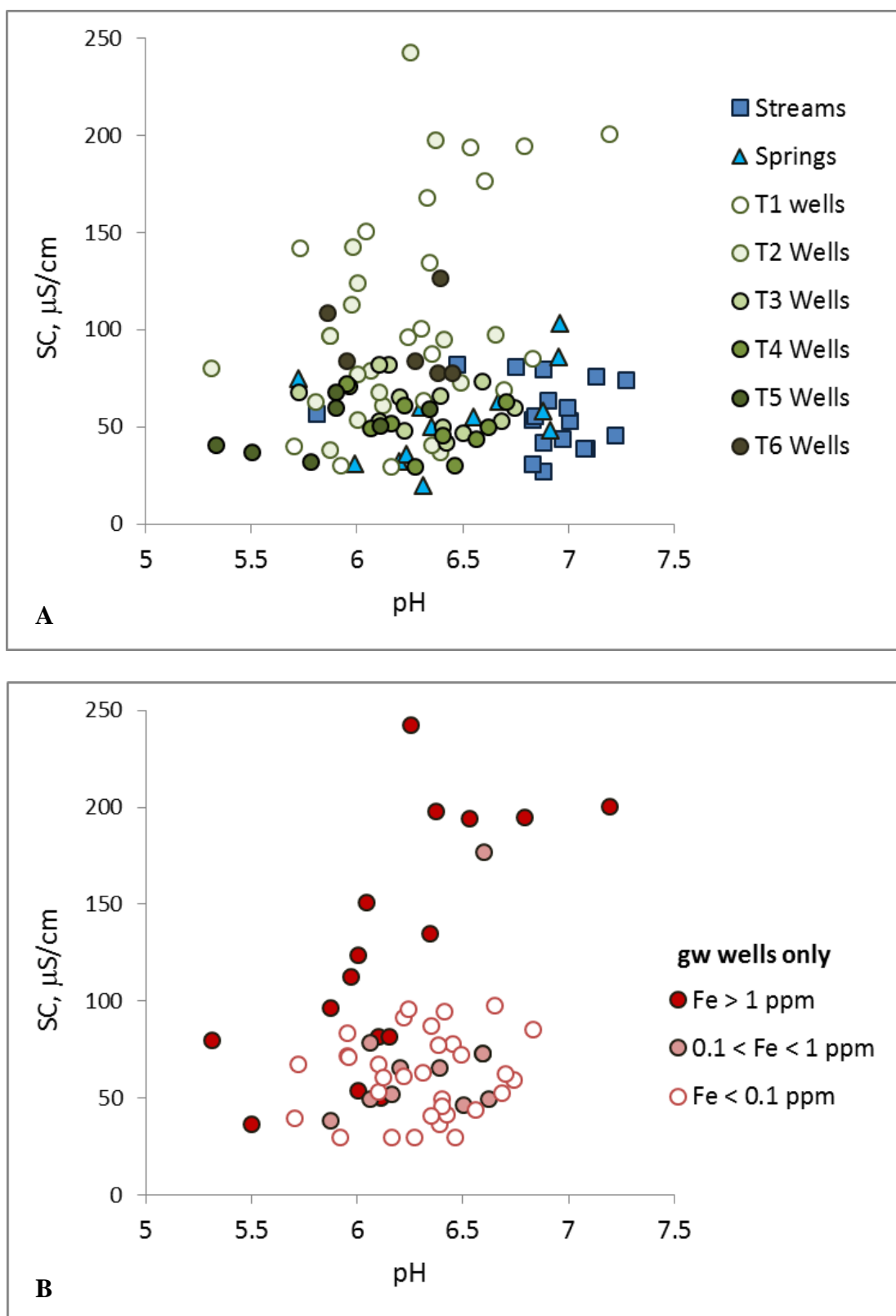
Figure 14: SC vs pH Diagrams

4.2. Carbonate Mineral Saturation Indicies

Chemical equilibrium modeling using Visual Minteq software helped determine the saturation state of minerals in groundwater samples. Parameters including pH, temperature, alkalinity and solute concentrations were used to design a chemical model. Figure 15 below shows results for carbonate minerals including calcite ($CaCO_3$), siderite ($FeCO_3$), and rhodochrosite ($MnCO_3$). This figure shows that all groundwater samples were strongly undersaturated with calcite, which also indicates that calcite would primarily be absent within the soils since it would dissolve in the presence of groundwater.

Several of the samples plotted in Figure 15 are close to equilibrium with siderite (S.I. values within ± 0.3 log units of 0.0). The precipitation of siderite probably exerts an upper limit to the concentrations of dissolved Fe^{2+} that can be present in the high-SC groundwater. This assumes equilibrium and does not take into account possible kinetic barriers to nucleation and growth of siderite. Rhodochrosite exhibits intermediate S.I. values between those of calcite and siderite. Although the groundwaters are undersaturated with pure rhodochrosite, it is possible that Mn-rich siderite could have exerted a solubility control (upper limit) on dissolved Mn^{2+} concentrations. This is because the solubility of Mn^{2+} as an impurity in $FeCO_3$ should be quite a bit less than that of pure $MnCO_3$.   Natural siderites often contain Mn as an impurity.   It would be interesting to test this idea by careful analysis of the mineralogy of the soil, but this was outside the scope of this study.
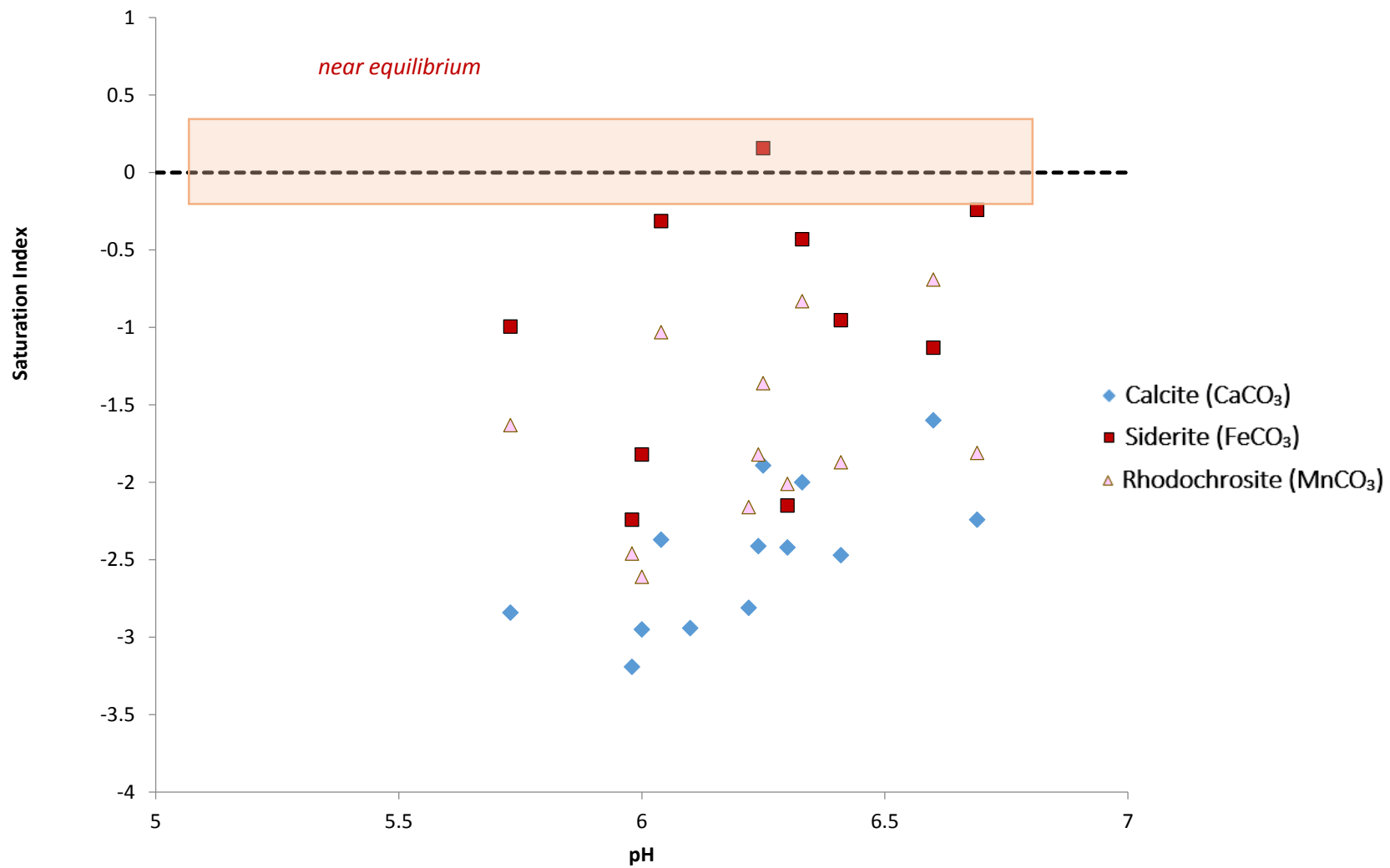
Figure 15: Computed saturation indices for calcite, siderite, and rhodochrosite for samples collected in July, 2013 and July, 2014.

4.3.   General Controls on the Isotopic Compositions of DIC and DOC

The following discussion, which follows basic principles outlined in Clark and Fritz (1997), outlines the processes that combine to produce the observed $\delta^{13}C$ values in the streams and groundwater samples of this study. To begin with, atmospheric CO_2 is globally well-mixed, with an average $\delta^{13}C$ near -7 ‰ (VPDB). Most terrestrial plants in temperate climates have a C_3 metabolism, and uptake ^{13}C slower than ^{12}C during photosynthesis.   As a result, the organic carbon in plant matter is strongly depleted in ^{13}C, with values ranging from -24 to -30 ‰ (global average of -27 ‰, Clark and Fritz, 1997). The $\delta^{13}C$ composition of DOC in groundwater collected in this study ranged from -28.1 to -32.7 ‰ (average = -31.1±1.4‰, error is one standard deviation). Thus, the range in $\delta^{13}C$-DOC from the study area overlaps with the typical values of $\delta^{13}C$ of C_3 plants reported by Clark and Fritz.

Microbial respiration converts organic carbon in the decaying plant matter to inorganic carbon with very little isotopic fractionation. Thus, CO_2 formed from respiration should have $\delta^{13}C$ between -24 to -30 ‰. However, because CO_2 concentrations in soils are typically orders of magnitude higher than in air (see Figure 13), some CO_2 is constantly diffusing out of the soil zone. And, because diffusion is faster for $^{12}CO_2$ vs. $^{13}CO_2$, the CO_2 pool that is left behind in the soil becomes slightly heavier. Clark and Fritz (1997) state that, for these reasons, soil gas in temperate climates typically has $\delta^{13}C$ near -23 ‰. Dissolution of CO_2 gas into water has about a 1‰ fractionation, resulting in dissolved CO_2 of soil water that is poised near -24‰.

Clark and Fritz's value of -24‰ for dissolved CO_2 is quite a bit lighter than most of the $\delta^{13}C$-DIC values obtained in this study. Based on data tabulated in Appendix E, the average $\delta^{13}C$-DIC value for groundwater samples in this study is -17.3 ± 2.3‰ (n = 50). However, there is a big difference between $\delta^{13}C$-CO_2 and $\delta^{13}C$-DIC. This is because of the large isotopic

fractionation that exists between dissolved CO_2 (usually written as H_2CO_3) and bicarbonate ion,

HCO_3^-. In this study, the concentrations of H_2CO_3 and HCO_3^- were calculated using Visual

Minteq based on the field-measured values of pH, temperature, and alkalinity. Because the

isotope analyses give $\delta^{13}C$ of total DIC, it is a simple mass balance problem to solve for the

isotopic compositions of H_2CO_3 and HCO_3^-, individually:

$$\delta^{13}C\text{-}HCO_3^- \cdot [HCO_3^-] \ + \ \delta^{13}C\text{-}H_2CO_3 \cdot [H_2CO_3] \ = \delta^{13}C\text{-}DIC \cdot [DIC] \qquad (V)$$

where the brackets [ ] indicate molal concentration. In the above equation, all of the

concentrations are known and $\delta^{13}C$-DIC is known. Furthermore, $\delta^{13}C$-HCO_3^- and $\delta^{13}C$-H_2CO_3

are related by the equilibrium isotopic separation, Δ, as follows:

$$\delta^{13}C\text{-}HCO_3^- - \delta^{13}C\text{-}H_2CO_3 \ = \Delta \qquad (VI)$$

After substituting equation VI into equation V, the following algebraic solution is obtained:

$$\delta^{13}C\text{-}HCO_3^- \ = \ \delta^{13}C\text{-}DIC + \Delta \cdot [H_2CO_3]/[DIC] \qquad (VII)$$

Values of Δ were calculated for the temperature of each sample based on data in Clark and Fritz

(1997), and averaged close to 10‰. Once the isotopic composition of HCO_3^- was found, the

isotopic composition of H_2CO_3 was simply $\delta^{13}C$-HCO_3^- - Δ.

Following the method outlined above, concentrations and isotopic compositions of

H_2CO_3 and HCO_3^- were calculated for each water sample in this study. The results, tabulated in

Appendix E, give a range in $\delta^{13}C$-H_2CO_3 for shallow groundwater in Stringer Creek of -18.0 to -

26.3 ‰, with an average value (n = 50) of -22.4 ± 1.8‰. This result is close to Clark and Fritz's

suggested value of -24 ‰ for biogenic CO_2 in "typical" soil water. Our data are also in

agreement with the measured values of $\delta^{13}C$ of CO_2 in soil gas samples collected from upper

Stringer Creek by other workers, most of which fall between -20 and -25 ‰ (Riveros-Iregui et

al., 2012).

A plot of δ^{13}C-DIC of groundwater vs. DIC concentration (Figure 16) shows a general

negative slope, implying that as DIC concentration increases, its isotopic composition becomes

more depleted. This trend is consistent with production of biogenic CO_2 via respiration. The

lower limit to how light the total DIC can get is set at the δ^{13}C of biogenic CO_2 prior to diffusive

loss, which should be around -25 to -30‰. Overall, the data in Figure 16 suggest that respiration

is the dominant metabolic process in the shallow groundwater, although there may be some

evidence for methanogenesis in some samples (see next section).
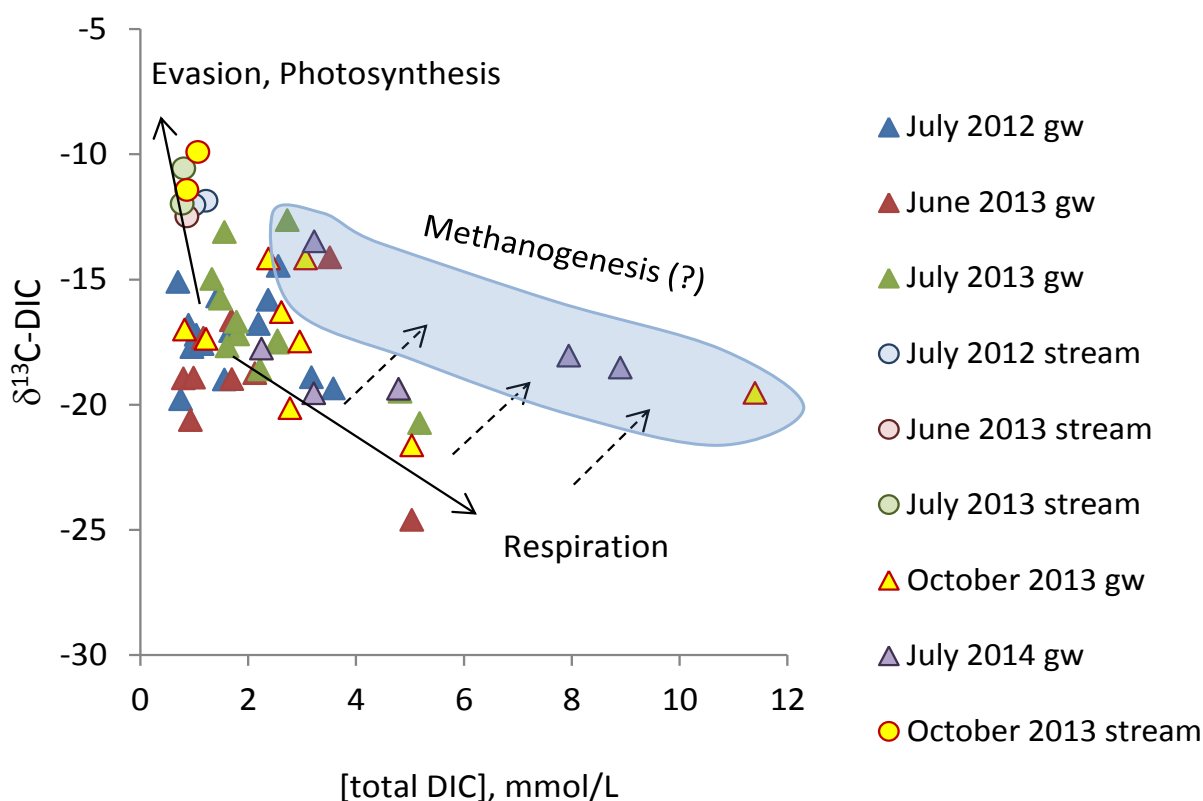
Figure 16: Isotopic DIC and DIC concentration. Triangles are groundwater (GW) samples. Circles are stream samples. Solid arrows show schematic trends for respiration, evasion, and photosynthesis. Dashed lines show schematic trends for acetoclastic methanogenesis.

The δ^{13}C-DIC of stream samples collected in this study were consistently heavier than

the groundwater samples. Based on data tabulated in Appendix E, the average value of δ^{13}C-

DIC for Stringer Creek and tributaries was -11.5 ± 0.9 ‰ (n = 7). When groundwater enters

Stringer Creek, the high partial pressure of dissolved CO_2 causes H_2CO_3 to diffuse out of the stream and into the air. This causes a drop in DIC concentration and a shift in $\delta^{13}C$-CO_2 and $\delta^{13}C$-DIC to heavier values. These trends are well displayed for the data from Stringer Creek ("stream" data in Figure 16). Day-time consumption of CO_2 by photosynthesizing aquatic plants can also result in an increase in $\delta^{13}C$ of the residual DIC. Recent workers have shown large diel changes in the concentration and isotopic composition of DIC in streams in Montana due to the 24-h cycle of respiration and photosynthesis (e.g., Parker et al., 2005, 2010). Although this could be tested at Stringer Creek, it was outside the scope of this thesis. Given the relatively low productivity of Stringer Creek, it is unlikely that the diel change in $\delta^{13}C$-DIC could have been very large (Parker et al., 2010).

4.4.   Stable Isotope Evidence for Methanogenesis

One of the main objectives of this thesis was to test whether or not methanogenesis, which is known to be important in the shallow wetland soil of Stringer Creek (Riveros-Iregui et al., 2012; Seybold et al., 2012), imparts a characteristic signal to the measured $\delta^{13}C$ of dissolved inorganic carbon. In a recent study of the biogeochemical evolution of a shallow Montana lake under ice cover (Gammons et al., 2014), the transition from respiration-dominant to methanogenesis-dominant metabolism was accompanied by a shift in the trend of $\delta^{13}C$-DIC vs. [DIC] from a negative slope (respiration) to a positive slope (methanogenesis). Figure 17 below, taken from the Gammons et al. (2014) study, shows these trends. The explanation for the positive slope is that acetoclastic methanogenesis produces equal moles of isotopically light CH_4 and isotopically heavy DIC (Whiticar et al., 1986; Whiticar, 1999), as shown by the following reaction:

$$CH_3COO^- \text{ (acetate)} + H_2O \rightarrow CH_4 \text{ (methane)} + HCO_3^- \qquad (VIII)$$
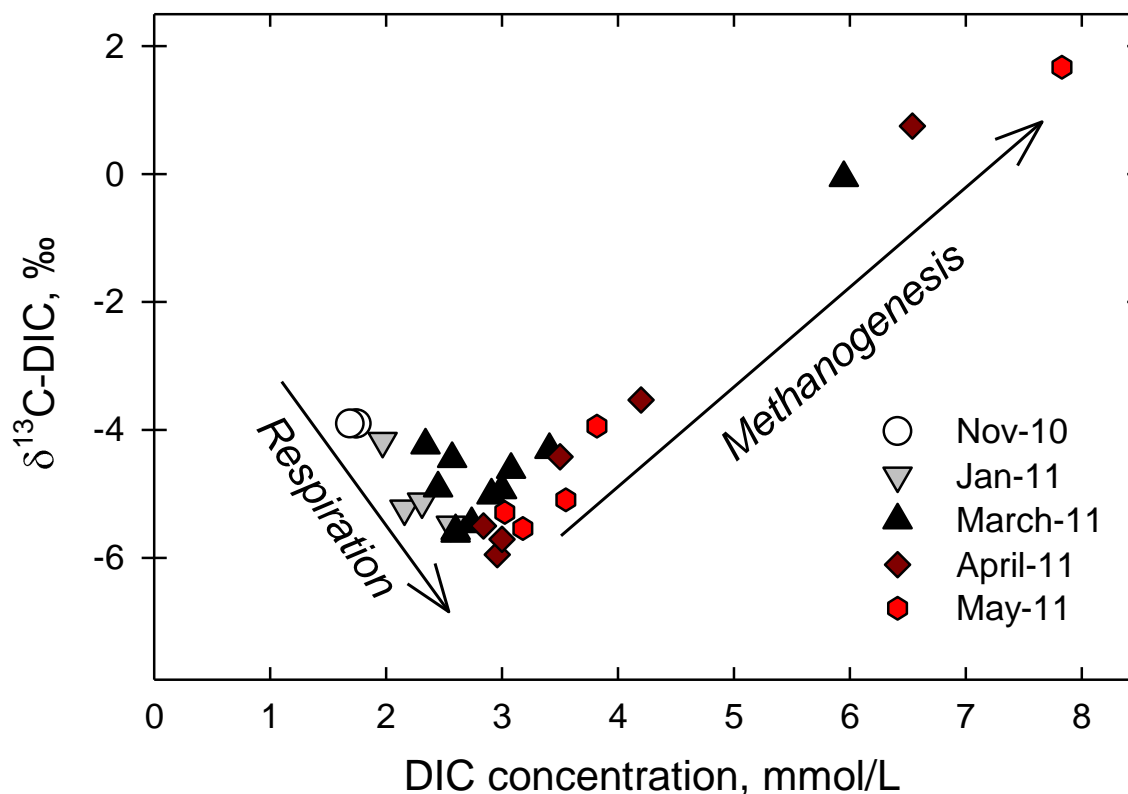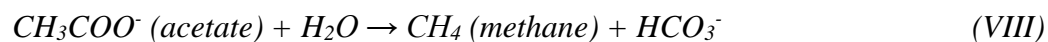
Figure 17: DIC isotope trends from Georgetown Lake (Gammons et al., 2014) showing the contrasting effect of respiration vs. methanogenesis

Following this idea, it was expected that some groundwater samples at Stringer Creek may show a similar shift in slope to more (+) values of δ^{13}C-DIC during times of the year when methanogenesis was a dominant process. An examination of the data in Figure 16 shows a scattering of well samples with high DIC concentration and anomalously high δ^{13}C-DIC. These wells were all from the wetland areas, with T1W1 being the single well that consistently showed higher [DIC] and δ^{13}C-DIC than the other wells (data in Appendix E). Supporting the idea that this could be a methanogenic signal, T1W1 had some of the highest dissolved CH_4 concentrations (up to 53.8 µmol/L) as determined from samples collected in July and October of 2013 (data in Table III of Results section). In contrast, sample T1E1, which also had high

dissolved CH_4 concentrations (up to 39.6 μmol/L), didn't show any evidence of isotopic enrichment in DIC.

Further isotopic evidence of methanogenesis is provided by the results of the peeper samples collected in 2014. The data, summarized in Figure 18A and 18B, show very little trend for Peeper 1. However, a nice trend of increasing δ^{13}C-DIC with both increase in depth (Figure 18C) and increase in total DIC concentration (Figure 18B) is displayed for the data of Peeper 2. Peeper 2 was placed into the Fe-rich boggy area immediately upstream (and on the west side) of Transect 1. The data set from Peeper 2 also shows a very strong increase in dissolved Fe^{2+} concentration with depth (Figure 10A of Results section). An interesting possibility to consider is that methanogenesis is somehow linked to reductive dissolution of Fe-oxides in this bog. Perhaps the CH_4 that is being produced is the source of DOC for Fe-respiring bacteria.
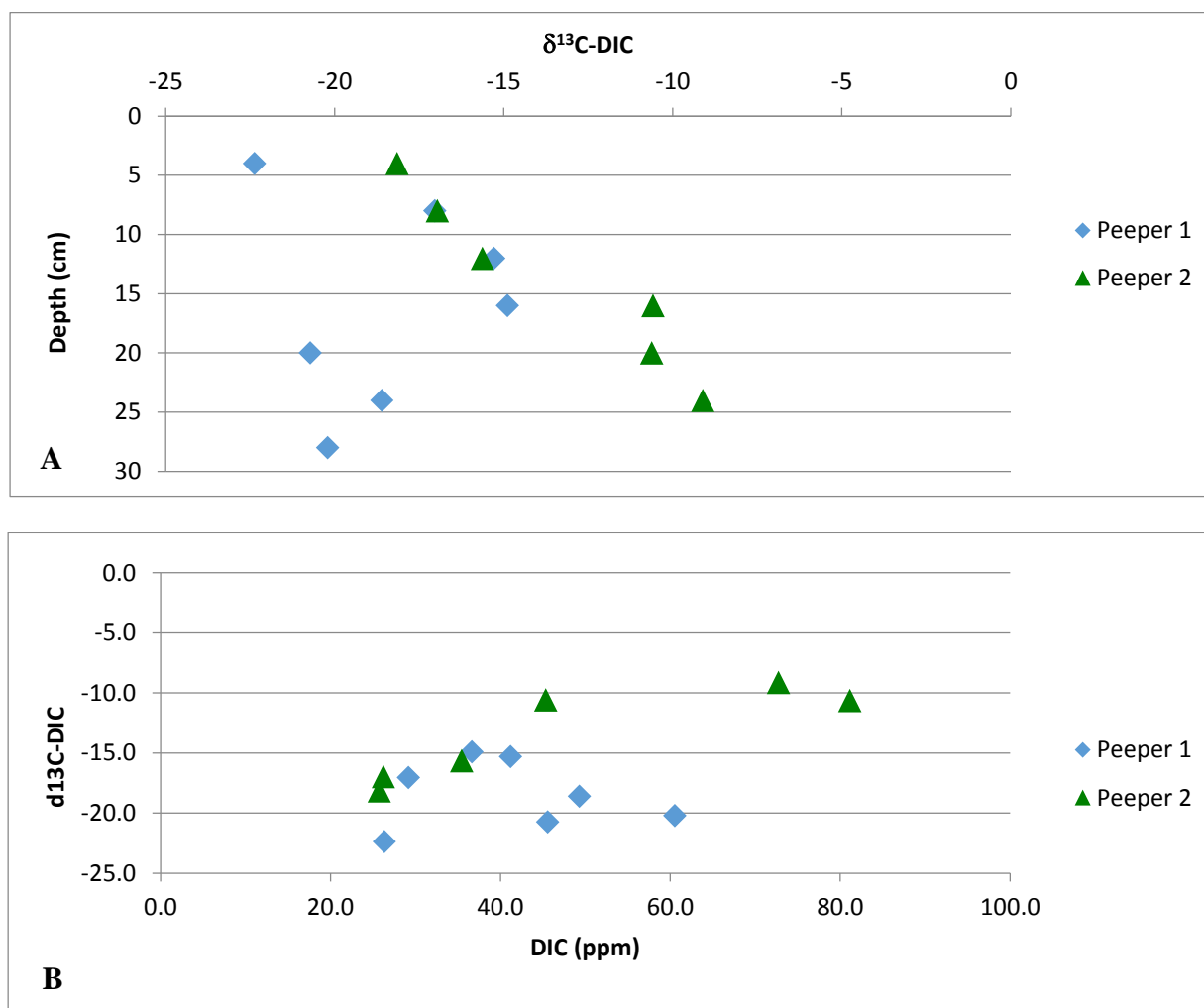
Figure 18: DIC Isotope Depth Profile from Peepers 1 & 2 collected in 2014

4.5. Implication of Sampling Problems to the Data Interpretation

Before too many inferences are made based on the C-isotope data of this thesis, it is

important to point out some possible side-reactions that could have happened during sampling

and storage of the DIC isotope samples. The main problem that probably created a lot of scatter

in the results is loss of $CO_2(g)$ during pumping and filtering of the groundwater samples. To

minimize loss of CO_2 during pumping, the wells were pumped at as slow of a rate as was

practical. More of a concern, however, is the fact that it often took 10+ minutes to filter the raw

water sample into the DIC isotope bottles. Some CO_2 likely escaped during this process,

although it is very hard to quantify this effect. Another potentially serious problem is that many of the wells (and peeper samples) with high dissolved Fe precipitated Fe-oxide in the DIC isotope bottles during storage. This reaction releases protons which, in the tightly sealed bottles, would have reacted with HCO_3^- to form CO_2, as shown by the following overall reaction:

$$Fe^{2+} + 2HCO_3^- + \tfrac{1}{4} O_2 + \tfrac{1}{2} H_2O \rightarrow Fe(OH)_3(s) + 2CO_2 \qquad (IX)$$

Shifting the form of DIC from HCO_3^- to CO_2 shouldn't change the $\delta^{13}C$ value of the bulk DIC in a closed system. However, because of the abundant colloidal $Fe(OH)_3$, these samples had to be re-filtered before isotopic analysis, and this additional step could have caused an additional loss of CO_2. Some direct evidence of CO_2-loss during sampling and processing was discovered late in this project. Namely, for the groundwater samples collected in the last field season, the total DIC concentrations computed based on the field pH-alkalinity-temperature readings were consistently higher than the DIC concentrations measured by the Picarro isotope analyzer.

Because CO_2 is lighter in $\delta^{13}C$ by about 10 ‰ compared to HCO_3^-, loss of CO_2 from the sample would have caused the $\delta^{13}C$-DIC of total DIC to drift to more positive values. Unfortunately, it is not possible to quantify this problem or back-correct the isotopic data collected in this thesis. Due to the very fine-grained, clay- and organic-rich nature of the wetland soils at Stringer Creek, the groundwater samples were extremely hard to pump, and even harder to filter. Even the peeper cell samples were hard to filter, something that has not been noted by the Montana Tech research group during installation and sampling of peepers at other field sites (C. Gammons, pers. communication). If further research of this type is done at Stringer Creek, additional research may be needed to come up with a sampling method that avoids the problem of CO_2 loss during filtering.

5. Conclusions and Recommendations

Below are some of the main conclusions based on the work in this thesis. This is followed by a short list of recommendations for further work.

5.1. Conclusions

- Shallow groundwater in the riparian corridor of upper Stringer Creek has higher total dissolved solids, slightly lower pH, and higher pCO$_2$ compared to the creek water itself.

- The increase in pH from groundwater to surface water is explained by evasion of CO$_2$ to the atmosphere. Some uptake of CO$_2$ by aquatic plants could also have occurred, although diel changes in pH and dissolved oxygen were generally of low amplitude in Stringer Creek, indicating a low level of aquatic productivity.

- Several wells in waterlogged wetland soil had highly elevated concentrations of Fe^{2+} and Mn^{2+}. However, no H$_2$S was detected in any of the wells.

- A sediment pore-water sampler (peeper) deployed in a boggy area with visible Fe seepage showed a rapid increase in concentration of Fe^{2+}, Mn^{2+}, and HCO$_3^-$ with depth in the first 30 cm of the wetland soil.

- Eh-pH diagrams computed via the STABCAL program indicate that the redox state of the shallow groundwater was poised near the aqueous Fe^{2+}/ferrihydrite boundary, with some samples approaching saturation with siderite (FeCO$_3$).

- Visual Minteq modeling suggests that all of the groundwater samples were undersaturated with respect to calcite and Mn-bearing solids, but approached equilibrium with siderite.

- Elevated levels of dissolved methane were observed in several groundwater wells, especially in the wetland areas, and is attributed to acetoclastic methanogenesis.

- In general, the groundwater data show a decrease in $\delta^{13}C$ with increase in DIC concentration, consistent with anaerobic or aerobic respiration being the dominant metabolic process in the wetland soil. However, several wells with high DIC concentration had slightly heavier $\delta^{13}C$ values. These same wells had elevated concentrations of dissolved methane, Fe^{2+}, and Mn^{2+}. These wells may have been influenced by acetoclastic methanogenesis, which produces isotopically light methane and isotopically heavy DIC.

- One of the peeper samplers showed a possible correlation between an increase in dissolved Fe^{2+} and an increase in $\delta^{13}C$-DIC. This type of trend would not be expected by anaerobic respiration of organic matter alone, and suggests a possible link between methanogenesis and Fe-reduction.

- The results of this study are complicated by the fact that it was exceedingly difficult to pump and filter water from the shallow groundwater wells in upper Stringer Creek. In particular, loss of dissolved CO_2 during filtering may have skewed some of the $\delta^{13}C$ results to heavier values.

5.2. Recommendations

- Given the difficulties encountered in this study, it would be a good idea to investigate alternative methods of extracting and filtering turbid groundwater that would avoid complications related to loss of dissolved CO_2.

- It might be interesting to characterize the mineralogy of the Fe-rich wetland soil to see what are the dominant Fe-minerals.

- An exploratory study could be conducted to investigate linkages between acetoclastic methanogenesis and Fe-reduction.

- More peeper sampling is recommended. This method proved to be relatively simple and avoided problems related to pumping of wells, although it was still difficult in some cases to filter the water in the peeper cells.

6. References

Clark I. D. and Fritz P. (1997) Environmental Isotopes in Hydrogeology. Lewis Publishers, NY.

Conrad R. (1996) Soil microorganisms as controllers of atmospheric trace gases (H2, CO, CH4, OCS, N2O, and NO). Microbiological Reviews 60:609-640.

Craig H. (1961) Isotopic variations in meteoric waters. Science 133:1702-1703.

Drever J.I. (1997) The Geochemistry of Natural Waters. 3rd ed., Prentice-Hall, Upper Saddle River, N.J.

Epstein S. and Mayeda T. (1953) Variation of O-18 content of waters from natural sources. Geochim. Cosmochim. Acta 4:213–224.

Farnes, P. E., Shearer, R. C., McCaughey, W. W., & Hanson, K. J. (1995). Comparisons of hydrology, geology and physical characteristics between Tenderfoot Creek Experimental Forest (east side) Montana, and Coram Experimental Forest (west side) Montana: Final Report RJVA-INT-92734. Forestry Sciences Laboratory. Bozeman, Mont.

Gammons C.H., Poulson S.R., Pellicori D.A., Roesler A., Reed P.J., Petrescu E.M. (2006) The hydrogen and oxygen isotopic composition of precipitation, evaporated mine water, and river water in Montana, USA. J Hydrol 328:319-330.

Gammons C.H., Henne W., Poulson S.R., Parker S.A., Johnston T., Dore J., Boyd E. (2014) Stable isotopes track biogeochemical processes under ice cover in a shallow, productive lake. Biogeochemistry 120, 359-379.

Gustafsson J. P. (2010) Visual MINTEQ, ver. 3.0, beta. http://www2.lwr.kth.se/English/OurSoftware/vminteq/

Harris D., Porter L.K., Paul E.A. (1997) Continuous flow isotope ratio mass spectrometry of carbon dioxide trapped as strontium carbonate. Commun Soil Sci Plant Analysis 28:747-757.

Hesslein R.H. (1976) An in situ sampler for close interval pore water studies. Limnology and Oceanography 21, 912-914.

Huang H. (2010) STABCAL user's manual, Montana Tech, Butte, Montana.

Jencso, K.G., B.L. McGlynn, M.N. Gooseff, S.M. Wondzell, K.E. Bencala, and L.A. Marshall (2009) Hydrologic connectivity between landscapes and streams:Transferring reach and plot scale understanding to the catchment scale, Water Resources Research, doi:10.1029/2008WR007225.

McCaughey, W.W. (1996). Tenderfoot Creek Experimental Forest. United States Department of Agriculture Forest Service General Technical Report Int, 101-108.

Morrison J., Brockwell T., Merren T., Fourel F. and Phillips A.M. (2001) On-line high precision stable hydrogen isotopic analyses on nanoliter water samples. Anal. Chem. 73:3570–3575.

Pacific, V.J., McGlynn, B.L., Riveros-Iregui, D.A., Welsch, D.L., Epstein, H.E. (2008). Variability in soil respiration across riparian-hillslope transitions. Biogeochemistry 91:51-70.

Pacific, V.J. (2009). Hydrology and landscape structure control subalpine catchment carbon export (Doctoral dissertation, Montana State University-Bozeman, College of Agriculture).

Parker S.R., Poulson S.R., Gammons C.H., and DeGrandpre M. (2005) Biogeochemical controls on diel cycles in the stable isotopic composition of dissolved O2 and DIC in the Big Hole River, Montana, USA. Environmental Science and Technology 39 (18): 7134-7140.

Parker S.R., Gammons C.H., Poulson S.R., DeGrandpre M.D., Weyer C.L., Smith M.G., Babcock J.N., Oba Y. (2010) Diel behavior of stable isotopes of dissolved oxygen and dissolved inorganic carbon in rivers over a range of trophic conditions, and in a mesocosm experiment. Chemical Geology 269:22-32.

Reynolds, M. (1995). Geology of Tenderfoot Creek Experimental Forest, Little Belt Mountains, Meagher County, Montana. Hydrologic and geologic characteristics of Tenderfoot Creek Experimental Forest, Montana, Final Rep. RJVA-INT, 92734, 21-32.

Riveros-Iregui, D.A., Liang, L., Emanuel, R.E., McGlynn, B.L., Dore, J., Kaiser, K., Seybold, E., and Covino, T.P. (2012) Soil carbon transformation in heterogeneous landscapes. AGU Fall 2012 Meeting Abstracts, p. 541.

Seybold E.C., Kaiser K., McGlynn B.L., Dore J.E., Riveros-Iregui D., Emanuel, R.E., Liang L., Covino T.P. (2012) Trace gas fluxes in complex terrain: The space-time dynamics of soil methane, carbon dioxide, and nitrous oxide. AGU Fall 2012 Meeting Abstracts, p. 540.

Smith M.G., Parker S.R., Gammons C.H., Poulson S.R., Hauer F.R. (2011) Tracing dissolved O2 and dissolved inorganic carbon stable isotope dynamics in the Nyack aquifer: Middle Fork Flathead River, Montana, USA. Geochim Cosmochim Acta 75:5971-5986.

Experimental Forest. U.S. Dept. Agriculture, Forest Serv. Retrieved September 9, 2014, from http://www.fs.fed.us/rm/tenderfoot-creek/

Whiticar, M.J., Faber, E., Schoell, M. (1986) Biogenic methane formation in marine and freshwater environments: CO2 reduction vs. acetate fermentation—Isotope evidence. Geochim Cosmochim Acta 50:693-709.

Whiticar, M.J. (1999) Carbon and hydrogen isotope systematics of bacterial formation and oxidation of methane. Chem Geol 161:291-314.

Wiesenburg D.A., Guinasso N.L. Jr (1979) Equilibrium solubilities of methane, carbon monoxide and hydrogen in water and sea water. J Chem Eng Data 24:356-360.

Appendix A: Field Parameter Data

Location	Date/time	Temp °C	pH SU	SC μS/cm	Eh mV, SHE	DO % sat	DO ppm	Alkalinity mg/L CaCO$_3$
July 9-10, 2012 Conditions: Moderately high water, good weather								
T1W1	7/10/2012 9:45	10.9	7.19	201	174	3.5	0.11	110
T1Stream	7/9/2012 16:00	9.6	5.81	57	213	103	9.1	n.a.
T1W2	7/10/2012 10:15	10.9	6.83	85.5	220	62.5	5	60
T1E1	7/10/2012 10:35	10.6	6.34	135	200	10.5	0.8	80
T1E2	7/10/2012 11:10	9.0	6.31	63.6	230	85.3	6.4	46
T2W2	7/9/2012 17:20	11.3	n.a.	192	n.a.	9.7	0.8	n.a.
T2W3	7/10/2012 12:30	11.4	6.49	73	255	41	3.5	42
T2W1	7/10/2012 11:50	8.6	6.37	198	220	13	1.21	72
T2E2	7/10/2012 13:30	n.a.	6.12	61	317	82	7.2	35
T2E1	7/10/2012 13:00	n.a.	6.65	98	307	52.3	4.6	53
T2Creek	7/10/2012 13:00	11.8	6.84	55.8	286	105.8	9.43	44
West Fork	7/10/2012 14:00	12.9	7.08	39	269	105	9.1	32
T3W1	7/10/2012 15:30	n.a.	6.74	60	289	51	4.27	32
T3E1	7/10/2012 15:30	13.4	6.50	47	329	71	6.01	20
T3E2	7/10/2012 16:00	n.a.	6.68	53	292	78	7.06	33
T4W1	7/10/2012 19:30	11.2	6.70	63	334	41.6	3.74	37
T4E1	7/10/2012 19:45	9.6	6.62	50	341	74.5	7.01	21
T4E2	7/10/2012 20:00	8.05	6.56	44	312	85	8.39	25
T4Creek	7/10/2012 18:00	15	7.00	53	214	106	8.74	n.a.
Flume	7/10/2012 17:00	9.96	6.90	64	308	100	9.35	37
July 30, 2012: Conditions: Low water, good weather								
T6E2	7/30/2012 9:50	11.3	5.86	109	n.a.	40	3.8	n.a.
T6E1	7/30/2012 10:10	7.18	5.95	84	n.a.	70	6.9	39
T6stream	7/30/2012 10:20	8.26	6.47	82	n.a.	95	9.4	40
T6W1	7/30/2012 10:40	9.9	6.27	84	n.a.	59	5.6	43
T5W2	7/30/2012 12:30	n.a.	5.50	37	n.a.	46	3.6	n.a.
T5E2	7/30/2012 14:00	n.a.	5.90	68	n.a.	75	6	n.a.
T5W1	7/30/2012 13:30	n.a.	n.a.	n.a.	n.a.	n.a.	n.a.	30
Tenderfoot	n.a.	9.4	6.88	80	n.a.	93	9	n.a.
Stringer mouth	n.a.	7.9	6.75	81	n.a.	93	9.3	n.a.

Appendix A: Field Parameter Data (Continued)

Location	Date/time	Temp °C	pH SU	SC µS/cm	Eh mV, SHE	DO % sat	DO ppm	Alkalinity mg/L CaCO$_3$
June 8-9, 2013 Conditions: Melting snow, high water table, many springs								
HWspring1	6/8/2013 9:30	4.2	6.31	20	386	100	n.a.	n.a.
HWspring2	6/8/2013 9:30	2.95	6.55	55	385	100	n.a.	n.a.
HWspring3	6/8/2013 9:30	2.9	6.67	63	387	100	n.a.	n.a.
HWspring4	6/8/2013 9:30	3.8	6.91	48	384	100	n.a.	n.a.
HWspring5	6/8/2013 9:30	5.5	6.20	32	392	96	n.a.	n.a.
T1W2	6/8/2013 10:00	6.41	5.92	30.2	395	66	6.3	10
T1W1	6/8/2013 10:59	7.63	6.79	195	191	27	2.5	120
T1E1	6/8/2013 13:00	7.8	5.70	40	324	19	1.65	40
T1E2	6/8/2013 11:54	6.53	6.16	30	334	88.4	8.39	13
T1Creek	6/8/2013 13:20	6.69	8.01	44	287	108	9.82	n.a.
T2W3	6/8/2013 1:55	7.01	6.35	41	339	65.9	6.15	46
T2W2	6/9/2013 0:00	9.3	6.06	79	334	71	n.a.	27
T2W1	6/9/2013 0:00	9.43	6.00	54	273	25.2	2.23	62
T2E1	6/9/2013 0:00	8.62	5.87	38.4	326	28	2.51	31
T2E2	6/8/2013 0:00	5.65	6.39	37	296	99.2	9.6	26
T2Creek	6/8/2013 16:00	8.75	6.97	44	316	108	9.63	39
Wfork	6/8/2013 16:30	10.2	6.83	31	308	102	8.85	n.a.
Etrib	6/8/2013 16:40	6.67	6.88	42	333	102	9.7	n.a.
T3W1	6/9/2013 10:10	7.72	6.40	50	334	39	3.66	23
T3E1	6/9/2013 10:30	7.37	6.22	48	284	25	2.3	46
T3E2	6/9/2013 0:00	6.15	6.42	42	335	66	6.3	23
T4W1	6/8/2013 18:00	5.31	6.40	46	377	62	6.1	38
T4E1	6/8/2013 18:00	3.20	6.27	30	251	46.7	4.48	43
T4E2	6/8/2013 19:00	3.60	6.46	30.2	271	95.3	9.74	40
T4Creek	6/8/2013 0:00	7.64	7.07	39.1	359	101	9.34	35
T4Eseep	6/8/2013 0:00	3.20	5.99	31	393	36	3.68	11
Spring below T4	6/9/2013 13:00	5.91	6.88	58.4	307	111.9	10.8	42

Appendix A: Field Parameter Data (Continued)

Location	Date/time	Temp °C	pH SU	SC µS/cm	Eh mV, SHE	DO % sat	DO ppm	Alkalinity mg/L CaCO$_3$
July 26-28, 2013 Conditions: Hot, dry, low water								
T2W3	7/26/2013	21	6.1	68	276	20.7	1.4	40
T1W1	7/27/2013 10:00	14.7	6.6	177	204	11.2	0.88	84
T1W2	7/27/2013 9:28	15.7	6.24	96.5	358	70.3	5.41	50
T1E1	7/27/2013 10:34	14.4	6.04	151	190	12.5	1	79
T2Stream	7/27/2013 11:00	7.7	6.99	60	234	99.7	9.25	30
T2W1	7/27/2013 13:10	13.3	6.25	243	133	6.2	0.49	99
T2E1	7/27/2013 14:50	18.6	6.41	95	281	30.7	2.6	39
T3E1	7/27/2013 14:40	14.7	6.1	82	250	12.7	1	n.a.
T3E2	7/27/2013 15:20	10.1	6.1	53.5	313	66	5.7	40
T3W1	7/27/2013 14:10	14.4	6.2	65.7	274	17	1.33	n.a.
T6W2	7/27/2013 15:40	17	6.39	127	170	91.8	6.92	n.a.
T6W1	7/27/2013	13.9	6.45	78.2	292	57.2	4.6	41
T6E1	7/27/2013	14.1	6.38	77.7	370	81.8	6.49	n.a.
T5W4	7/27/2013	13.15	5.78	32.2	321	65.4	5.34	n.a.
T5W3	7/27/2013	14.91	5.33	41	268	3.6	0.3	n.a.
T5W2	7/27/2013	14.47	6.11	50.5	297	9.3	0.72	n.a.
T5W1	7/27/2013	9.54	5.9	60	251	26.8	2.36	n.a.
T5E1	7/27/2013	14.05	6.34	59.1	258	69.2	5.82	n.a.
West Fork Seeps W	7/28/2013 10:00	8.99	7.22	46	409	98.6	8.8	21
below flume Seeps above	7/28/2013 10:23	4.14	6.96	103	438	93	9.5	45
T5	7/28/2013 10:30	4.17	6.3	60	444	86	8.73	28.5
Seeps at T5	7/28/2013	5.25	6.23	36	424	89.9	8.9	23
Bedrock well	7/28/2013 16:00	10.6	6.56	73.2	306	85.5	7.4	38
HWSpringNW	7/28/2013	5.21	6.35	50.1	373	84.4	8.3	21
HWSpringNE	7/28/2013	12.11	6.95	86	351	80.2	6.68	46
T5Creek	7/28/2013 11:21	6.63	7.27	74.5	271	99.4	9.47	35
T4W1	7/28/2013 12:07	11.77	6.22	61.3	359	29.3	2.49	31
T4E1	7/28/2013 12:35	n.a.	6.06	49.6	282	9.3	0.8	n.a.
T4E2	7/28/2013 13:00	10.34	6.16	52.1	250	68.7	5.92	31
T3W1	7/28/2013 14:40	14.7	6.39	66.1	314	63.2	5	45

Appendix A: Field Parameter Data (Continued)

Location	Date/time	Temp °C	pH SU	SC µS/cm	Eh mV, SHE	DO % sat	DO ppm	Alkalinity mg/L CaCO$_3$
October 5-6, 2013 Conditions: Cold, clear, recent snow, ice forming in creek								
Bedrock well	10/5/2013 10:30	5.93	6.22	92	344	69.6	6.72	42
T1Creek	10/5/2013 11:00	1.5	6.88	27	n.a.	n.a.	n.a.	30
West Fork	10/5/2013 12:00	1.47	6.83	54	542	96.3	11.4	23
T4Creek	10/5/2013 15:30	0.86	7.13	76	339	101	11.3	46
T4E1 Seep	10/5/2013 10:30	3.56	5.72	75	305	n.a.	n.a.	29
T1W2	10/6/2013 10:40	6.33	6.35	87.7	366	68	6.54	26
T1W1	10/6/2013 11:10	7.85	6.53	194.4	275	14.4	1.35	83
T1E1	10/6/2013 11:38	8.45	5.87	96.9	309	26	2.41	52
T1E2	10/6/2013 10:30	n.a.	n.a.	n.a.	n.a.	n.a.	n.a.	n.a.
T2W3	10/6/2013 10:30	n.a.	n.a.	n.a.	n.a.	n.a.	n.a.	n.a.
T2W2	10/6/2013 10:30	10.29	5.97	112.9	238	19.5	1.7	n.a.
T2W1	10/5/2013 13:12	8.39	6.00	124.3	203	8.2	0.75	36
T2E1	10/5/2013 12:41	7.49	5.31	80.2	389	25.2	2.73	37
T2E2	10/6/2013 11:38	8.45	5.87	96.9	309	26	2.41	52
T3W2	10/6/2013 13:44	n.a.	n.a.	n.a.	n.a.	n.a.	n.a.	n.a.
T3W1	10/6/2013 13:37	9.37	6.59	73.4	245	27	2.41	24
T3E1	10/6/2013 14:13	8.88	6.15	82.2	249	28.5	2.57	n.a.
T3E2	10/5/2013 14:32	7.30	5.72	68	413	42	3.98	n.a.
T4W1	10/5/2013 15:45	3.78	5.95	72.3	352	47.8	4.9	32
T4E1	10/6/2013 16:40	n.a.	n.a.	n.a.	n.a.	n.a.	n.a.	n.a.
T4E2	10/5/2013 16:15	2.41	5.96	71.4	289	70.3	7.56	28
July 27-28, 2014: Warm, sunny, low water								
T1W1	7/28/2014 12:15	17.12	6.33	168.4	329	8.1	0.63	61
T1W2	7/28/2014 12:40	20.20	6.30	100.5	322	50.3	3.55	43
T1E1	7/28/2014 11:45	19.34	5.73	142.2	354	13.2	0.95	53
T1E2	7/28/2014 11:35	17.02	6.69	69.5	330	41.8	3.11	46
T2W3	7/28/2014 9:25	15.20	6.00	77.1	336	14.2	1.14	36
T2W1	7/28/2014 10:05	11.82	5.98	142.6	331	9.5	0.96	96
T2E1	7/28/2014 10:26	14.85	5.80	63.3	378	44.6	3.54	39

Appendix B: ICP-AES Results

Samples Collected in July 2012

Sample ID	Ca mg/L	Mg mg/L	Na mg/L	K mg/L	Fe mg/L	Mn mg/L	Si mg/L	SO$_4$[1] mg/L
PQL[2]	0.1	0.1	0.5	0.5	0.08	0.001	0.1	0.3
T1W1	21.8	8.2	2.7	0.6	1.65	0.825	5.1	11.6
T1W2	9.5	2.8	2.0	0.8	<0.08	0.018	4.3	9.8
T1E1	12.1	3.5	1.5	<0.5	10.70	0.804	5.7	0.9
T1E2	6.7	1.8	1.1	0.6	<0.08	0.078	4.6	1.3
FLUME	7.9	2.5	1.2	0.5	<0.08	<0.001	5.0	2.6
West fork	5.4	1.2	1.2	<0.5	<0.08	<0.001	4.1	1.9
T2 CREEK	7.5	2.1	1.1	<0.5	<0.08	0.002	5.1	1.7
T2E2	7.1	2.8	1.2	0.7	<0.08	0.080	4.4	2.9
T2E1	11.5	4.8	1.9	0.6	<0.08	0.016	6.5	5.2
T2W3	9.1	2.7	1.7	<0.5	<0.08	0.006	4.9	6.8
T2W1	13.8	4.1	2.3	<0.5	4.11	0.100	5.1	4.9
T3W1	7.7	2.2	1.6	0.6	<0.08	0.010	5.2	1.8
T3E1	6.7	2.0	1.1	<0.5	0.57	0.059	5.7	1.4
T3E2	6.7	2.0	1.1	<0.5	<0.08	<0.001	5.2	1.5
T3E2-D	6.6	2.0	1.1	<0.5	<0.08	<0.001	5.1	1.4
T4W1	7.2	2.2	1.2	0.5	<0.08	0.040	4.7	1.9
T4E1	5.2	1.3	1.2	<0.5	0.13	0.028	4.3	1.8
T4E2	5.8	1.5	1.0	0.5	<0.08	<0.001	4.3	1.9
T5W1	6.1	2.5	1.5	0.6	0.06	0.009	5.8	2.5
T5W2	3.9	1.5	1.4	<0.5	1.54	0.027	5.7	3.5
T5W3	4.9	2.0	1.7	<0.5	2.36	0.033	5.5	1.9
T5E1	7.6	3.3	1.3	0.7	<0.08	0.001	4.9	3.7
T6W1	9.5	4.5	1.4	0.7	<0.08	0.026	4.9	4.0
T6 CREEK	9.2	3.9	1.4	0.5	<0.08	<0.001	4.7	4.2
T6E1	9.7	4.3	1.3	0.7	<0.08	<0.001	4.6	3.6

[1]Calculated from ICP-AES analysis for S, assumes all S is SO_4^{2-}; [2]Practical quantification limit

Appendix B: ICP-AES Results (Continued)

Samples Collected in June 8-9, 2013

Sample ID	Ca mg/L	Mg mg/L	Na mg/L	K mg/L	Fe mg/L	Mn mg/L	SO$_4$[1] mg/L
PQL[2]	0.1	0.1	0.5	0.5	0.08	0.001	0.3
Headwater seep	8.0	2.1	1.2	0.6	0.16	0.003	1.6
T1E1	5.6	1.7	1.1	<0.5	0.78	0.379	1.5
T1E2	3.7	1.0	0.9	<0.5	<0.08	0.001	1.4
T1W1	22.2	9.4	2.8	0.5	4.14	1.028	13.7
T1W2	3.7	1.1	1.3	<0.5	<0.08	0.004	2.0
T2E2	4.3	1.8	0.9	0.5	<0.08	0.006	1.6
T2E1	31.0	17.1	17.5	2.5	0.09	0.017	0.2
T2 Creek	5.6	1.5	1.1	<0.5	<0.08	<0.001	1.4
T2W1	7.6	2.3	1.8	<0.5	1.27	0.047	3.5
T2W2	8.4	2.7	2.4	<0.5	0.12	0.093	11.8
T2W3	5.0	1.6	1.4	<0.5	<0.08	<0.001	1.8
T3E2	5.1	1.6	1.1	<0.5	<0.08	<0.001	1.6
T3W1	6.1	1.9	1.3	<0.5	<0.08	0.011	1.6
T4E Seep	3.8	1.0	1.0	0.8	<0.08	<0.001	1.5
T4E2	3.8	1.0	1.0	<0.5	<0.08	<0.001	1.4
T4E1	3.8	1.0	1.0	<0.5	<0.08	<0.001	1.4
T4 Creek	4.9	1.4	1.1	<0.5	<0.08	<0.001	1.4
T4W1	6.0	1.8	1.2	<0.5	<0.08	0.003	2.3

[1]Calculated from ICP-AES analysis for S, assumes all S is SO_4^{2-}; [2]Practical quantification limit

Appendix B: ICP-AES Results (Continued)

Samples Collected July 26-28, 2013

Sample ID	Ca mg/L	Mg mg/L	Na mg/L	K mg/L	Fe mg/L	Mn mg/L	SO$_4$[1] mg/L
PQL[2]	0.1	0.1	0.5	0.5	0.08	0.001	0.3
Headwater NE Seep	11.9	3.4	1.5	0.5	<0.08	0.012	2.4
Headwater NW Seep	6.7	1.6	1.5	0.6	<0.08	<0.001	3.1
T1- Bedrock	8.9	2.5	1.4	0.9	<0.08	0.002	2.4
T1W2	11.2	3.9	2.7	1.2	<0.08	0.168	13.4
T1E1	13.5	4.2	1.9	<0.5	16.4	1.124	2.1
T1W1	22.5	9.3	3.1	0.8	0.72	0.697	16.4
T2E1	11.3	5.0	2.4	0.7	<0.08	0.011	5.8
T2W1	22.1	7.0	3.3	<0.5	26.4	0.284	3.6
T2W3	9.9	3.1	2.2	<0.5	<0.08	0.004	10.0
T2 Stream	8.2	2.6	1.4	<0.5	<0.08	0.004	2.5
West Trib	6.2	1.5	1.5	<0.5	<0.08	<0.001	2.7
T3E1	7.4	2.3	1.5	<0.5	2.86	0.098	1.8
T3E2	6.5	2.1	1.4	<0.5	<0.08	<0.001	2.0
T3W1	8.6	2.7	1.7	0.6	0.20	0.064	2.9
T4E1	5.4	1.4	1.4	0.6	0.16	0.069	2.4
T4W1	8.3	2.6	1.6	0.6	<0.08	0.138	2.8
T4 East Seep	6.1	1.6	1.3	0.5	<0.08	0.001	2.5
T4E2	6.8	1.8	1.4	0.6	0.24	0.011	2.3
T4.5 flume seep	11.1	6.2	1.9	0.8	<0.08	<0.001	9.0
T5W2	4.4	1.6	1.6	<0.5	1.22	0.008	2.7
Seep above T5	6.5	3.0	1.6	0.6	<0.08	<0.001	4.8
Seep at T5W2	3.7	1.6	1.5	0.5	<0.08	<0.001	2.7
T5 Creek	8.6	3.7	1.5	0.6	<0.08	<0.001	4.8
T6W1	8.5	4.3	1.6	0.7	<0.08	0.018	4.3
T6E1	8.9	4.1	1.6	0.8	<0.08	0.001	4.0

[1]Calculated from ICP-AES analysis for S, assumes all S is SO$_4^{2-}$; [2]Practical quantification limit

Appendix B: ICP-AES Results (Continued)

Samples Collected October 5-6, 2013

Sample ID	Ca mg/L	Mg mg/L	Na mg/L	K mg/L	Fe mg/L	Mn mg/L	Si mg/L	SO$_4$[1] mg/L
PQL[2]	0.1	0.1	0.5	0.5	0.08	0.001	0.1	0.3
T1 Creek	10.0	2.9	1.4	0.6	<0.08	0.004	4.8	3.4
T1E1	7.8	2.3	1.3	<0.5	1.23	0.448	4.3	1.9
T1W1	20.9	7.9	2.6	0.6	1.65	0.939	4.7	13.5
T1W2	9.5	3.0	8.6	0.7	<0.08	0.048	3.6	12.6
Bedrock	11.7	3.4	1.6	0.8	<0.08	0.001	4.3	3.1
T2E1	8.5	3.6	1.9	0.5	2.97	0.129	7.7	5.4
T2W1	10.4	3.2	2.7	<0.5	4.07	0.050	4.1	15.1
T2W2	11.4	3.5	2.6	<0.5	1.04	0.135	4.6	28.5
West Trib	6.7	1.6	1.5	0.6	<0.08	<0.001	4.0	5.0
T3E1	8.1	2.4	1.4	0.3	2.74	0.157	5.7	2.5
T3E2	8.2	2.5	1.4	0.4	<0.08	<0.001	4.7	3.5
T3W1	8.5	2.5	1.3	0.5	0.10	0.027	4.2	4.6
T4 Creek	9.3	2.9	1.5	0.6	<0.08	<0.001	3.9	5.2
T4E1	9.4	2.3	1.5	1.3	2.39	0.248	5.2	2.1
T4E2	8.6	2.2	1.4	0.6	<0.08	<0.001	4.2	3.5
T4W1	8.7	2.6	1.5	0.5	<0.08	0.056	4.3	3.8
T4E seep	8.5	2.2	1.4	0.8	<0.08	0.028	4.1	3.5

[1]Calculated from ICP-AES analysis for S, assumes all S is SO$_4$$^{2-}$; [2]Practical quantification limit

Samples Collected July 27-28, 2014

Sample ID	Ca mg/L	Mg mg/L	Na mg/L	K mg/L	Fe mg/L	Mn mg/L	Si mg/L	SO$_4$[1] mg/L
PQL[2]	0.1	0.1	0.5	0.5	0.08	0.001	0.1	0.3
T1W1	19.4	7.7	2.9	0.5	7.80	1.127	5.1	11.6
T1W2	10.4	3.5	2.5	0.9	0.21	0.104	4.2	9.6
T1E1	14.2	4.5	1.9	b.d.	11.6	0.890	5.5	1.2
T2W1	19.4	6.0	3.0	b.d.	20.8	0.200	6.5	1.5
T2W3	7.58	2.4	2.1	0.6	1.11	0.064	4.8	7.5
T2E1	6.62	2.9	2.1	0.7	0.63	0.135	6.9	5.6
T1-Stream	7.38	2.1	1.3	b.d.	b.d.	0.003	5.0	1.6
T1-StreamDup	7.40	2.1	1.3	b.d.	b.d.	0.003	5.1	1.6

[1]Calculated from ICP-AES analysis for S, assumes all S is SO$_4$$^{2-}$; [2]Practical quantification limit

Appendix B: ICP-AES Results (Continued)

"*Peeper 0*" sampled July 30, 2012

Depth	Ca	Mg	Na	K	Fe	Mn	Si	SO$_4$[1]
cm	mg/L	mg/L	mg/L	mg/L	mg/L	mg/L	mg/L	mg/L
PQL[2]	0.3	0.3	1.5	1.5	0.2	0.003	0.3	1.0
2	11.4	3.3	1.6	<1.5	1.2	0.037	14.8	7.4
6	11.8	3.2	1.6	<1.5	2.4	0.017	13.4	2.6
10	12.1	3.3	1.6	<1.5	1.8	0.007	13.0	5.9
14	12.4	3.5	1.7	<1.5	1.7	0.017	13.0	5.4
18	11.0	3.0	<1.5	2.0	1.9	0.015	21.5	2.7
22	12.8	3.6	1.6	3.0	2.1	0.015	13.5	5.0
26	13.7	3.7	1.6	3.5	3.7	0.032	13.6	2.7

[1]Calculated from ICP-AES analysis for S, assumes all S is SO$_4^{2-}$; [2]Practical quantification limit

"*Peeper 1*" sampled Aug. 11, 2014

Depth	Ca	Mg	Na	K	Fe	Mn	Si	SO$_4$[1]	PO$_4$[2]
cm	mg/L	mg/L	mg/L	mg/L	mg/L	mg/L	mg/L	mg/L	mg/L
PQL[3]	0.3	0.3	1.5	1.5	0.2	0.003	0.3	1.0	0.3
6	6.0	1.5	<1.5	<1.5	1.1	0.04	5.6	<1.0	<0.3
14	11.9	2.8	2.6	<1.5	5.9	0.11	5.8	1.9	<0.3
18	26.5	6.1	3.8	<1.5	12.5	0.22	6.1	2.8	0.7
22	28.0	6.4	4.0	<1.5	11.9	0.23	6.2	3.3	<0.3
26	26.2	5.9	3.8	<1.5	12.5	0.28	6.4	3.4	1.1

[1]Calculated from ICP-AES analysis for S, assumes all S is SO$_4^{2-}$; [2]Calculated from ICP-AES analysis for P, assumes all P is PO$_4^{3-}$; [3]Practical quantification limit

"*Peeper 2*" sampled Aug. 11, 2014

Depth	Ca	Mg	Na	K	Fe	Mn	Si	SO$_4$[1]	PO$_4$[2]
cm	mg/L	mg/L	mg/L	mg/L	mg/L	mg/L	mg/L	mg/L	mg/L
PQL[3]	0.3	0.3	1.5	1.5	0.2	0.003	0.3	1.0	0.3
2	12.9	3.4	<1.5.	<1.5	26.7	0.96	5.6	1.5	0.9
6	13.7	3.6	<1.5.	<1.5	31.5	1.47	5.9	1.4	0.7
10	15.4	3.9	<1.5	<1.5	31.3	3.45	6.1	1.4	<0.3
14	19.9	5.1	1.7	<1.5	53.4	2.52	7.4	1.7	0.7
18	25.3	6.3	<1.5	<1.5	98.0	2.28	9.9	2.4	2.9
22	40.1	9.7	3.5	<1.5	168.0	2.93	12.6	3.5	4.8
26	43.9	10.5	3.5	<1.5	147.0	3.41	10.8	3.1	1.8

[1]Calculated from ICP-AES analysis for S, assumes all S is SO$_4^{2-}$; [2]Calculated from ICP-AES analysis for P, assumes all P is PO$_4^{3-}$; [3]Practical quantification limit

Appendix C: Ion Chromatography (IC) Data

Samples Collected July 26-28, 2013

Sample ID	F mg/L	Cl mg/L	SO$_4$ mg/L	NO$_3$-N mg/L	PO$_4$-P mg/L
PQL[1]	0.0015	0.005	0.01	0.001	0.03
Upper seep, NE	0.059	0.074	1.84	0.026	<0.03
Upper seep, NW	0.047	0.18	2.68	0.013	<0.03
T1W1	0.24	0.32	14.6	0.009	<0.03
T1W1 (red)	0.096	0.049	1.43	0.001	<0.03
T1W2	0.075	0.33	11.0	0.020	<0.03
T1-bedrock	0.059	0.23	1.99	0.014	<0.03
T2E1	0.12	0.22	5.02	0.059	<0.03
T2W1 (red)	0.11	0.045	2.41	0.005	<0.03
T2W3	0.078	0.13	8.65	0.002	<0.03
T2-stream	0.053	0.13	2.05	0.003	<0.03
T3W1	0.061	0.15	2.39	0.007	<0.03
T3E2	0.053	0.15	1.68	0.002	<0.03
T4W1	0.061	0.27	2.25	0.027	<0.03
T4E2	0.049	0.20	2.05	<0.001	<0.03
T4.5 seep near flume	0.094	0.22	7.79	0.027	<0.03
T4 seep on east bank	0.046	0.13	2.11	0.001	<0.03
T6E1	0.064	0.26	3.43	0.048	<0.03
T6W1	0.077	0.19	3.72	0.022	<0.03
Seep above T5	0.062	0.18	4.18	0.007	<0.03
Seep at T5W2	0.052	0.15	2.30	<0.001	<0.03

[1]Practical quantification limit

Appendix C: Ion Chromatography (IC) Data (Continued)

Samples Collected July 27-28, 2014

Sample ID	F mg/L	Cl mg/L	SO$_4$ mg/L	NO$_3$-N mg/L	PO$_4$-P mg/L
PQL[1]	0.01	0.3	0.1	0.125	0.05
T1E1	0.16	<0.3	1.3	<0.125	<0.05
T2E1	0.23	0.4	5.5	<0.125	<0.05
T1Stream	0.04	<0.3	2.0	<0.125	<0.05
T1Stream DUP	0.06	<0.3	2.0	<0.125	<0.05
T1W1	0.17	<0.3	12.6	<0.125	<0.05
T1W2	0.06	<0.3	9.8	<0.125	<0.05
T2W1	0.14	<0.3	1.6	<0.125	<0.05
T2W3	0.09	<0.3	7.6	<0.125	<0.05

[1]Practical quantification limit

Appendix D: Water Isotope Data

Samples Collected July 2012

Sample ID	UNR[1] $\delta^{18}O$	UNR δD
T1E1	-19.4	-145
T1E2	-19.4	-145
T1W1	-19.4	-146
T1W2	-19.5	-146
T2E1	-19.1	-142
T2E2	-19.4	-145
T2W1	-19.3	-144
T2W3	-19.5	-147
T2 Creek	-19.4	-145
TRIB	-19.3	-145
T3E1	-19.3	-144
T3W1	-19.3	-144

[1] University of Nevada, Reno

Samples Collected June 2013

Sample ID	MBMG $\delta^{18}O$	MBMG δD	UNR $\delta^{18}O$	UNR δD
T3E2	-19.2	-147	-19.1	-146
T1E1	-19.5	-149	-19.3	-147
T4W1	-19.8*	-151*	-19.1*	-147*
T2Creek	-19.7	-150	-19.4	-147
T1W2	-19.8	-151	-19.6	-149
T1E2	-19.7	-150	-19.5	-148
T2E2	-19.8	-151	-19.6	-148
T2W1	-19.6	-151	-19.5	-149
T1W1	-19.5*	-149*	-18.9*	-145*
T2W3	-19.8	-152	-19.7	-150

[1] University of Nevada, Reno
[2] Montana Bureau of Mines and Geology
* Sample was evaporated

Appendix E: Carbon Isotope Data

Measured and calculated values for concentrations and isotopic compositions of total dissolved inorganic carbon (DIC), HCO_3^-, H_2CO_3, and $CO_2(g)$.   Units: mM = molal x 10^{-3}; matm = atmosphere x 10^{-3}

	measured		calculated					
	δ^{13}C-DIC	alkalinity	Total DIC	HCO_3^-	H_2CO_3	pCO_2	δ^{13}C-HCO$_3$	δ^{13}C-H$_2$CO$_3$
	‰ PDB	mg/L CaCO$_3$	mM	mM	mM	matm	‰ PDB	‰ PDB
Samples of July 2012								
T1E1	-19.4	80	3.58	1.60	1.98	37.5	-13.4	-24.2
T1E2	-16.8	46	2.19	0.92	1.27	22.8	-10.4	-21.4
T1W1	-14.5	110	2.56	2.20	0.36	7.28	-13.0	-23.7
T1W2	-17.1	60	1.68	1.20	0.48	9.16	-14.0	-24.7
T2E1	-15.8	53	2.37	1.06	1.31	24.9	-9.9	-20.6
T2E1-D	-16.3							
T2E2	-15.7	35	1.44	0.70	0.74	14.0	-10.2	-20.9
T2W1	-18.9	72	3.18	1.44	1.74	30.8	-12.9	-23.9
T2W3	-19.0	42	1.56	0.84	0.72	14.1	-14.1	-24.7
T3E1	-19.8	20	0.75	0.40	0.35	6.5	-14.7	-25.5
T3E2	-17.2	33	1.04	0.66	0.38	7.07	-13.3	-24.1
T3W1	-17.7	32	0.96	0.64	0.32	5.97	-14.1	-24.9
T4E1	-15.1	21	0.70	0.42	0.28	5.15	-10.8	-21.6
T4E2	-16.8	25	0.90	0.50	0.40	6.9	-11.9	-22.9
T4W1	-17.6	37	1.15	0.74	0.41	7.56	-13.7	-24.5
T5E1	-15.7	*a*	*a*	*a*	*a*	*a*	*a*	*a*
T5W1	-18.4	30	*b*	0.60	*b*	*b*	*b*	*b*
T6E1	-14.3	39	*b*	0.78	*b*	*b*	*b*	*b*
T6W1	-13.4	43	*b*	0.86	*b*	*b*	*b*	*b*
T2-Creek	-11.9	44	1.22	0.88	0.34	6.65	-8.9	-19.5
Creek at								
upper flume	-12.0	37	1.00	0.74	0.26	4.77	-9.2	-20.0
Samples of June 2013								
T1W1	-14.1	120	3.52	2.40	1.12	19.2	-10.6	-21.7
T1W2	-20.6	10	0.93	0.20	0.73	11.9	-11.8	-23.0
T1E1	-24.6	40	5.04	0.80	4.24	83.6	-15.6	-26.3
T1E2	-19.0	13	0.80	0.26	0.54	8.91	-11.4	-22.6
T2E2	-17.3	26	1.17	0.52	0.65	10.4	-11.1	-22.4
T2W3	-18.7	46	2.13	0.92	1.21	20.3	-12.4	-23.6
T3E2	-18.9	23	0.99	0.46	0.53	8.6	-12.9	-24.2
T4E2	-19.0	40	1.70	0.80	0.90	13.3	-12.9	-24.4
T4W1	-16.6	38	1.69	0.76	0.93	14.7	-10.4	-21.7
T4 creek	-18.6	11	0.96	0.22	0.74	10.8	-9.6	-21.3
T4E seep	-12.5	35	0.87	0.70	0.17	2.97	-10.3	-21.4

a = missing data due to insufficient sample mass for alkalinity measurement; b = missing data due to pH electrode malfunction

Appendix E: Carbon Isotope Data (Continued)

Measured and calculated values for concentrations and isotopic compositions of total dissolved inorganic carbon (DIC), HCO_3^-, H_2CO_3, and $CO_2(g)$.

	measured		calculated					
	$\delta^{13}C$-DIC ‰ PDB	alkalinity mg/L CaCO$_3$	Total DIC mM	HCO$_3^-$ mM	H$_2$CO$_3$ mM	pCO$_2$ matm	$\delta^{13}C$-HCO$_3$ ‰ PDB	$\delta^{13}C$-H$_2$CO$_3$ ‰ PDB
Samples of July 2013								
T1W1	-12.6	84	2.73	1.68	1.05	22.7	-8.7	-18.9
T1E1	-20.7	79	5.18	1.58	3.60	77.6	-13.6	-23.9
Bedrock	-15.0	38	1.33	0.76	0.57	10.8	-10.4	-21.1
T2W1	-19.5	99	4.82	1.98	2.84	58.9	-13.4	-23.8
T2W3	-18.6	40	2.22	0.80	1.42	37.7	-12.6	-22.0
T3W1	-17.2	45	1.81	0.90	0.91	19.9	-12.1	-22.3
T2E1	-15.8	39	1.49	0.78	0.71	17.3	-11.1	-20.9
T3E2	-17.4	40	2.55	0.80	1.75	32.6	-10.0	-20.8
T3E2-dup	-17.5	40	2.55	0.80	1.75	32.6	-10.1	-20.9
T4W1	-17.7	31	1.61	0.62	0.99	19.6	-11.2	-21.8
T4E2	-16.7	31	1.79	0.62	1.17	22.1	-9.7	-20.4
T6E1	-14.5	*a*	*a*	*a*	*a*	*a*	*a*	*a*
T6W1	-13.1	41	1.56	0.82	0.74	15.6	-8.2	-18.5
T2 stream	-12.0	30	0.78	0.60	0.18	3.06	-9.4	-20.5
T5 stream	-10.6	35	0.81	0.70	0.11	1.85	-9.0	-20.2
NE seep	-14.4	46	1.19	0.92	0.27	5.41	-12.0	-22.5
NW seep	-16.5	21	1.00	0.42	0.58	9.04	-9.9	-21.3
T4E seep	-16.7	*a*	*a*	*a*	*a*	*a*	*a*	*a*
T4.5W seep	-11.8	45	1.21	0.90	0.31	4.73	-8.8	-20.3
T5 seep	-14.6	28.5	1.48	0.57	0.91	13.8	-7.6	-19.1
Samples of October 2013								
T1E1	-21.6	52	5.04	1.04	4.00	70.6	-12.9	-23.9
T1W1	-14.2	83	3.07	1.66	1.41	24.4	-9.1	-20.1
T1W2	-17.4	26	1.22	0.52	0.70	11.4	-10.9	-22.2
Bedrock	-14.2	42	2.38	0.84	1.54	8.91	-11.4	-22.6
T2E1	-19.5	37	11.4	0.74	10.7	182	-9.2	-20.3
T2W1	-20.1	36	2.78	0.72	2.06	36.3	-12.0	-23.0
T3W1	-17.0	24	0.82	0.48	0.35	6.29	-12.5	-23.3
T3E2	-18.5	*a*	*a*	*a*	*a*	*a*	*a*	*a*
T4W1	-17.5	32	2.96	0.64	2.32	20.3	-12.4	-23.6
T4E2	-16.3	28	2.62	0.56	2.06	8.60	-12.9	-24.2
T1 creek	-11.4	30	0.87	0.60	0.27	3.71	-7.8	-19.6
T4 creek	-9.9	46	1.07	0.92	0.15	2.09	-8.2	-20.1
T4E seep	-18.7	29	4.17	0.58	3.59	53.0	-8.7	-20.3

a = missing data due to insufficient sample mass for alkalinity measurement

Appendix E: Carbon Isotope Data (Continued)

Measured and calculated values for concentrations and isotopic compositions of total dissolved inorganic carbon (DIC), HCO_3^-, H_2CO_3, and $CO_2(g)$.

	measured		calculated					
	$\delta^{13}C$-DIC ‰ PDB	alkalinity mg/L $CaCO_3$	Total DIC mM	HCO_3^- mM	H_2CO_3 mM	pCO_2 matm	$\delta^{13}C$-HCO_3 ‰ PDB	$\delta^{13}C$-H_2CO_3 ‰ PDB
Samples of July 2014								
T1W1	-13.5	61	3.23	1.22	2.01	26.4	-6.1	-18.0
T1W2	-17.8	43	2.25	0.86	1.39	20.6	-10.6	-22.2
T1E1	-18.0	53	7.95	1.06	6.89	92.0	-7.7	-19.6
T2W3	-19.5	36	3.22	0.72	2.50	33.7	-10.3	-22.2
T2W1	-18.5	96	8.9	1.92	6.98	93.2	-9.2	-21.1
T2E1	-19.4	39	4.79	0.78	4.01	59.2	-9.7	-21.3

Appendix F: Dissolved organic carbon data

Samples of October, 2013
These samples analyzed by MBMG lab using carbon analyzer

Location	DOC, mg/L
Bedrock well	0.2
T1Creek	0.7
T1W2	1.7
T1W1	0.7
T2W1	6.9
T2E1	1.2
T3E1	3.5
T3E2	1.0
T4W1	1.1
T4E1	5.6
T4E2	0.6
T4E Seep	0.9

Samples of July, 2014
These samples were analyzed by Steve Parker using Picarro C-isotope analyzer

Location	DOC, mg/L	δ^{13}C-DOC, ‰ VPDB
T1-Stream	1.0	-32.7
T1-Stream Dup	1.0	-31.8
T1E1	2.0	-28.1
T1W1	1.2	-32.0
T2W1	1.3	-31.5
T1W2	1.3	-30.6
T2E1	1.2	-30.4
T2W3	0.7	-31.5

Appendix G: Piper Diagram of 2012-2014 Groundwater Data
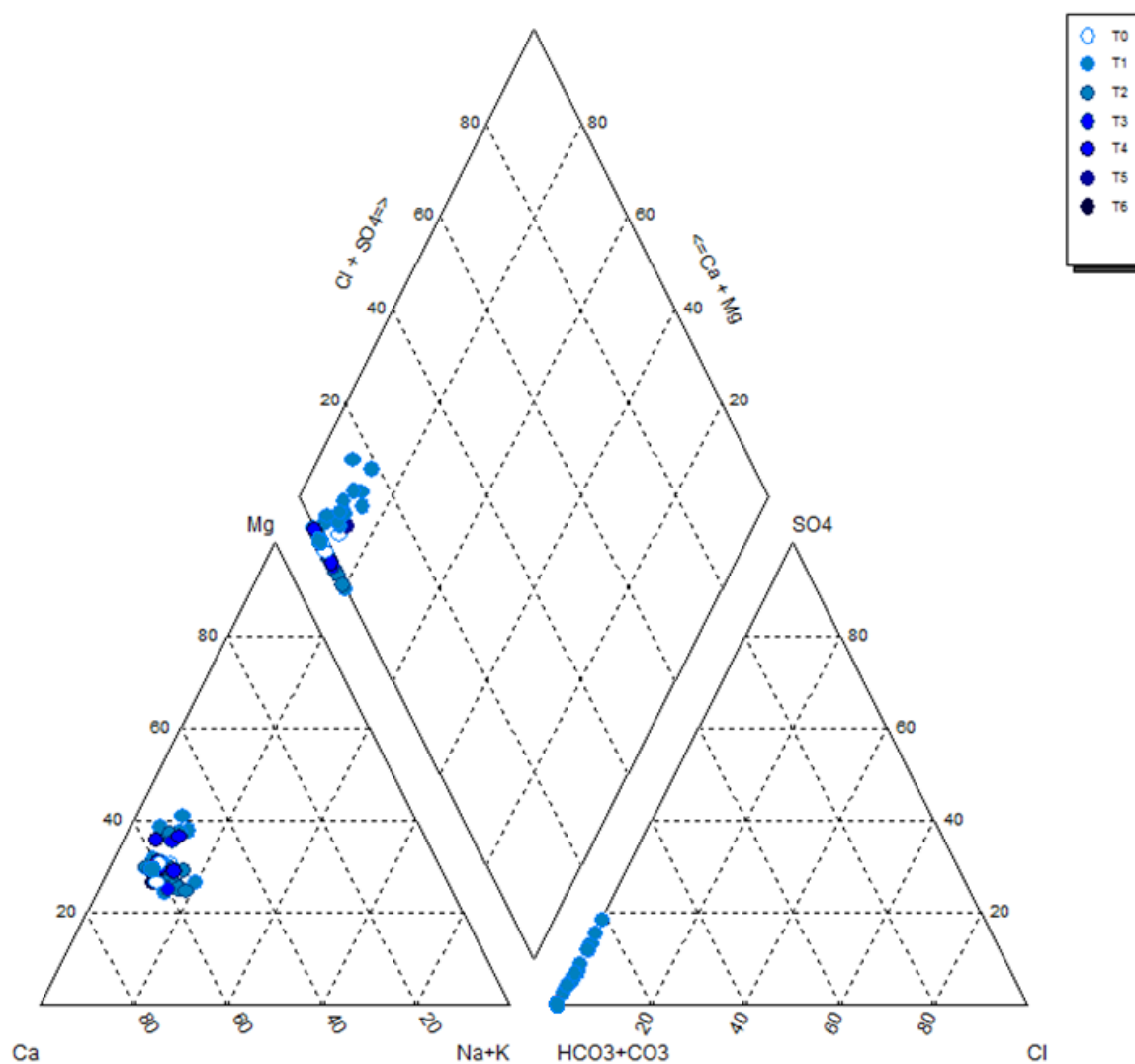
Chloride was not analyzed in the samples above, thus data on the bottom right plots along the HCO_3+CO_3 line. Additionally, the absence of Cl would also affect the middle diagram showing slight shifts towards the Cl + SO_4 side.
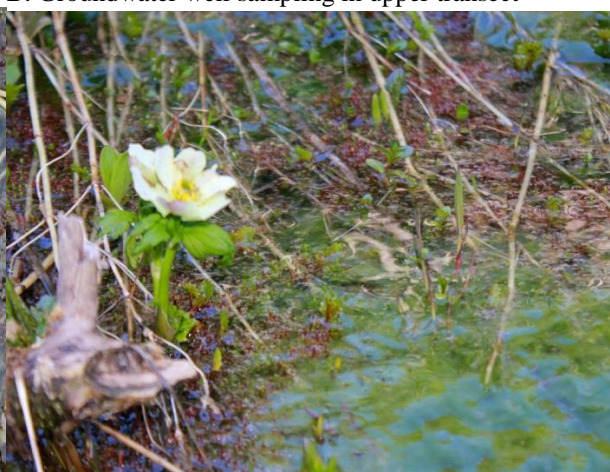
Appendix H: Photographs

A. Excited field technicians, ready to sample

B. Groundwater well sampling in upper transect

C. Gas bubble release from microbial interactions

D. Marshy seep near transect 6

E. Suite of peeper samples collected on site

F. Iron oxidation of groundwater at peeper site

G. Soil Water Filtration at Montana Tech

H. Soil extraction in the field

I. Groundwater lab sampling

J. Soil water experimentation and extraction

K. Bolete mushroom discovered at field site

L. Field assistants busy at work

M. Chris Gammons during an early sampling visit

N. Soil Processing at Montana Tech labratory

O. Stringer Creek above transect 1 in June 2013

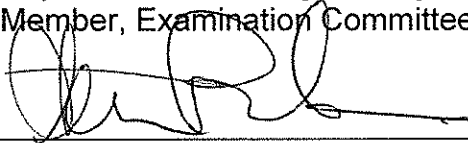P. Rock carin identifying a peeper sampling site

SIGNATURE PAGE

This is to certify that the thesis prepared by **Amanda Capri Gillam** entitled **"Biogeochemical Cycling in a Headwater Stream and Riparian Zone"** has been examined and approved for acceptance by the **Department of Geological Engineering**, Montana Tech of the University of Montana on this **17th day of April 2015**.

Dr. Christopher Gammons, Department Head & Professor
Department of Geological Engineering
Chairman, Examination Committee

Dr. Glenn D. Shaw, Associate Professor
Department of Geological Engineering
Member, Examination Committee

Dr. Steve Parker, Professor
Department of Chemistry & Geochemistry
Member, Examination Committee